NASA

Technical Memorandum 83904

Nuclear Processes in Solar Flares

R. Ramaty

MARCH 1982

National Aeronautics and
Space Administration

Goddard Space Flight Center
Greenbelt, Maryland 20771

NUCLEAR PROCESSES IN SOLAR FLARES

R. Ramaty

Laboratory for High Energy Astrophysics

NASA/Goddard Space Flight Center

Greenbelt, Maryland 20771

Chapter 3 in "The Physics of the Sun"

Edited by

T. E. Holzer

D. Mihalas

P. A. Sturrock

R. K. Ulrich

Abstract

The theory of solar gamma-ray line production is reviewed and new calculations of line production yields are presented. Observations, carried out with gamma-ray spectrometers on OSO-7, HEAO-1, HEAO-3 and SMM are reviewed and compared with theory. These observations provide direct evidence for nuclear reactions in flares and furnish unique information on particle acceleration and flare mechanisms.

I. INTRODUCTION

Nuclear reactions in solar flares take place between flare accelerated protons and nuclei and the ambient solar atmosphere. Several reviews of the early work on this subject are available (Dolan and Fazio 1965, Lingenfelter and Ramaty 1967, Cheng 1972). Using reasonably accurate and complete nuclear data, Lingenfelter and Ramaty (1967) have carried out the first detailed calculation of the expected nuclear reaction rates in flares and predicted observable fluxes at Earth of the products of these reactions, gamma-ray lines, neutrons and nuclear fragments in the solar energetic particles.

Nuclear gamma rays from solar flares were first observed by Chupp et al. (1973) with a NaI spectrometer flown on board the seventh Solar Orbiting Observatory (OSO-7). Gamma-ray lines at 0.51 MeV, 2.22 MeV, 4.44 MeV and 6.13 MeV were observed from the August 4, 1972 flare. The lines at 0.51 and 2.22 MeV were also seen during the decay phase of the August 7, 1972 flare. These two flares were among the largest ever observed.

A considerable amount of theoretical and interpretative work has been carried out on the August, 1972 observations (Ramaty and Lingenfelter 1973, Reppin et al. 1973, Wang and Ramaty 1974, Forrest, Chupp and Suri 1975, Ramaty, Kozlovsky and Lingenfelter 1975, Wang 1975, Kanbach et al. 1975, Chupp 1976, Lin and Hudson 1976, Bai and Ramaty 1976, Ramaty and Crannell 1976, Crannell et al. 1976, Kozlovsky and Ramaty 1977, Ramaty, Kozlovsky and Suri 1977 Ibragimov and Kocharov 1977, Lin and Ramaty 1978, Crannell, Crannell and Ramaty 1979, Ramaty 1979, Ramaty et al. 1980). These studies, together with additional gamma-ray data (Chupp, Forrest and Suri 1975, Chupp 1976, Suri et al. 1975), and energetic-particle (Kohl, Bostrom and Williams 1973, Webber et al. 1975), hard X-ray (van Beek, Hoyng and Stevens 1973) and microwave (Croom and Harris 1973) data have lead to the following broad outline of the origin

and implications of solar gamma rays.

Gamma-ray lines from solar flares result from the interaction of flare accelerated protons and nuclei with the solar atmosphere. The emission measure of flare heated material, i.e. the density squared of the hot gas times its volume which is determined from X-ray observations, is insufficient to produce any measurable amount of nuclear burning. The accelerated particles, on the other hand, produce neutrons, positrons, π mesons, radioactive nuclei and excited nuclear levels, whose captures, annihilations, decays, and deexcitations lead to observable gamma-ray lines.

The strongest line in solar flares is at 2.223 MeV from neutron capture on hydrogen. The neutrons are produced mainly from the disintegration of ^{4}He and heavier nuclei and occasionally in proton-proton collisions resulting in high-energy neutrons and π mesons. High-energy neutrons could be directly detected near Earth (Lingenfelter et al. 1965, Lingenfelter and Ramaty 1967) and preliminary reports of their observation have just become available (Chupp and Forrest 1981).

The site of the nuclear reactions in the solar atmosphere is as yet unknown. Nevertheless, calculations (Wang and Ramaty 1974) indicate that the bulk of neutrons with initial velocity vectors pointing towards the photosphere are thermalized in the photosphere and subsequently captured on either ^{1}H or ^{3}He. Capture on ^{1}H produces the 2.223 MeV gamma-ray line, but capture on ^{3}He results in tritium without emitting photons. The removal time of thermal neutrons from the photosphere, on the order of a minute, can be measured by comparing the time dependence of the intensity of the 2.223 MeV line to that of a prompt nuclear line (see below). This removal time depends on the photospheric ^{3}He abundance, as does the capture probability on ^{1}H which determines the flux of the 2.223 MeV line. Gamma-ray line observations,

therefore, can measure the abundance of ^{3}He in the photosphere. Because the 2.223 MeV line is formed at a larger depth in the solar atmosphere than the prompt gamma-ray lines, for flares close to the limb of the Sun, the 2.223 MeV line is substantially attenuated relative to the prompt emissions.

A variety of prompt gamma-ray lines are produced from nuclear deexcitations. The most important discrete lines (Ramaty, Kozlovsky and Lingenfelter 1975, 1979) are at 6.129 MeV from ^{16}O, 4.438 MeV from ^{12}C, 2.313 MeV from ^{14}N, 1.779 MeV from ^{28}Si, 1.634 MeV from ^{20}Ne, 1.369 MeV from ^{24}Mg, 1.238 MeV and 0.847 MeV from ^{56}Fe, all produced primarily by direct excitation of these nuclei, and at two lines, 0.478 MeV from ^{7}Li and at 0.431 MeV from ^{7}Be, which result from fusion reactions, ^{4}He(α,p)^{7}Li* and ^{4}He(α,n)^{7}Be*. The role of these fusion reactions for producing gamma-ray lines in astrophysics was first pointed out by Kozlovsky and Ramaty (1974). Nuclear deexcitations also produce Doppler broadened lines which together with many unresolved lines produce a significant gamma-ray continuum, in particular in the 4 to 7 MeV region (Ramaty, Kozlovsky and Suri 1977, Ibragimov and Kocharov 1977).

Because of the short lifetimes of most excited nuclear levels, nuclear deexcitation radiation is an excellent tracer of the nuclear interaction rate of energetic particles in solar flares. This rate is directly proportional to the instantaneous number of accelerated particles in the interaction region, which, in turn, is determined by the acceleration mechanism and the losses suffered by the particles. Through line shapes and Doppler shifts, prompt nuclear deexcitation lines also give information on the geometry of the interacting energetic particle beam (Ramaty and Crannell 1976, Kozlovsky and Ramaty 1977).

The interaction models of energetic protons and nuclei in solar flares can be crudely classified as thin- and thick-target models (e.g. Ramaty,

Kozlovsky and Lingenfelter 1975). In the thin-target model the nuclear reactions are produced by energetic particles which escape from the interaction region at the Sun. These particles can be detected in the interplanetary medium. Furthermore, if sufficient thin-target nuclear reactions take place, their fragmentation products should also be detectable. On the other hand, in the thick-target model the nuclear reactions are produced by particles as they slow down in the solar atmosphere. These particles, and their spallation products, become thermalized and mixed back into the solar atmosphere. Gamma-ray lines and neutrons can, nevertheless, be seen from thick-target interactions.

The ratio of the flux in a prompt nuclear component (e.g. the 4.44 MeV line) to the flux in the 2.223 MeV line depends on the interaction model and on the energy spectrum of the accelerated particles. For a given energetic particle spectrum, this ratio is larger for the thin-target than for the thick-target model. Using this result and information on the energy spectrum derived from interplanetary particle observations (Van Hollebeke, MaSung and McDonald 1975), Ramaty (1979) suggested that the gamma rays from the August 4, 1972 flare were produced predominantly in thick-target interactions. From the absolute fluxes of the gamma ray lines, it is possible to deduce the energy deposited by the accelerated nuclei in the solar atmosphere. For the August 4, 1972 flare, the energy deposited by the protons and nuclei amounts to several percent of the energy deposited by the electrons which make the impulsive hard X-rays (Lin and Hudson 1976). Nevertheless, protons could deposit their energy in regions which are not accessible to electrons because they have a longer stopping range in the ambient medium than the < 100 keV electrons.

Positrons in solar flares result from the decay of π^+ mesons and various

radioactive nuclei produced by the nuclear reactions. The half lives of the important positron emitters range from values less than 1 second to over 20 minutes and they produce positrons of energies from about 0.1 MeV to several tens of MeV. After their production, the positrons are decelerated to energies less than several hundred eV where they annihilate. The deceleration is due to interactions with the ambient solar atmosphere, and hence the deceleration time depends on the density and magnetic field of the medium in which the positrons annihilate. The positrons can annihilate with free electrons to produce two 0.511 MeV gamma rays per annihilation, or they may form a positronium atom. This atom is similar to the hydrogen atom except that the proton is replaced by a positron. Positronium atoms also annihilate into gamma rays: 25% of the annihilations are from the singlet spin state producing two 0.511 MeV photons, and 75% of them are from the triplet state which annihilates into three photons of energies less than 0.511 MeV. Triplet positronium can annihilate before it is broken up by collisions only if the density of the ambient medium is less than about 10^{15} cm^{-3}. Observation of the characteristic 3-photon positronium continuum, therefore, would provide information on the density of the annihilation site (Crannell et al. 1976). Information on the temperature of this site would be obtained from the measurement of the width of the 0.511 MeV line. If the positrons annihilate below the transition layer, i.e. at temperatures less than 10^5K, the width the 0.511 MeV line should be less than 3.5 keV.

Following the OSO-7 observations, solar gamma-ray lines were seen with the NaI spectrometer on the first High Energy Astrophysical Observatory (HEAO-1) (Hudson et al. 1980), with the NaI spectrometer on the Solar Maximum Mission (SMM) (Chupp et al. 1981, Chupp 1981), and with the Ge spectrometer on HEAO-3 (Prince et al. 1982). The two HEAO detectors, designed to detect

cosmic gamma rays, observed solar gamma-ray lines through their shields and thus were sensitive to only the strongest one or two lines. The HEAO detectors are no longer operational. The SMM spectrometer has already seen line emission from many solar flares and thus demonstrated that nuclear reactions of flare accelerated particles take place commonly in solar flares. At the time of this writing (early 1982) the detector is still operational and should continue to observe for several more years. The ten solar flares, from which gamma-ray lines were definitely seen so far, are discussed in the present paper.

In addition to gamma-ray lines and neutrons, nuclear reactions also produce energetic nuclear fragments (e.g. ^{2}H, ^{3}H, ^{3}He, Li, Be, B). The first attempt to measure the ^{3}He abundance in energetic solar particles was made by Schaeffer and Zahringer (1962). By using mass spectroscopy of material from the Discoverer 17 satellite, these authors found a $^{3}He/^{4}He$ ratio of ~ 0.2 for the November 12,1960 flare. Subsequent measurements (Hsieh and Simpson 1970, Anglin, Dietrich and Simpson 1973a, Dietrich 1973, Garrard, Stone and Vogt 1973) have revealed the existence of a class of solar particle events in which the $^{3}He/^{4}He$ ratio is substantially larger than in the ambient solar atmosphere.

Enrichments of ^{3}He in energetic particle populations (for example, the galactic cosmic rays) have been generally attributed to nuclear reactions between the energetic particles and the ambient medium. But, as first pointed out by Garrard, Stone and Vogt (1973), this interpretation of the solar ^{3}He enrichments, in its simplest form, is inconsistent with much of the ^{3}He data. If the ^{3}He enrichments are due to nuclear reactions of the energetic particles, then they should be accompanied by similar enrichments in ^{2}H and, to a lesser degree, in ^{3}H. Such enrichments, however, are not observed.

Several schemes have been proposed to overcome this difficulty. These rely on the kinematics and angular distributions of the reaction products which favor the preferential escape of ^{3}He (Ramaty and Kozlovsky 1974, Rothwell 1976) and the thermonuclear destruction of ^{2}H and ^{3}H in a model in which the energetic products of the nuclear reactions are confined to thin filaments and interact with each other (Colgate, Audouze and Fowler 1977). But, as proposed by Fisk (1978), the enhanced ^{3}He abundance in solar energetic particles could be due to preferential heating and acceleration of ambient atmospheric ^{3}He. The observation of energetic ^{3}He, therefore, cannot be used as indication for nuclear reactions unless the ^{3}He is accompanied by at least some other fragmentation product. No convincing observations of such products have yet been reported.

Nuclear reactions of accelerated particles could cause modifications of solar surface isotopic abundances. Thus, from the analysis of lunar surface material, Kerridge (1975) found a secular increase of the solar wind $^{15}N/^{14}N$ ratio, and Fireman, De Felice and D'Amico (1976) reported a measurable ^{14}C abundance on the lunar surface which they believe should be due to implantation by the solar wind. Even though solar surface nuclear reactions could, in principle, produce these isotopes, it is unlikely that this has indeed happened, because the necessary nuclear reaction rates on the ancient Sun would have to exceed the present rate (determined by the gamma-ray observations) by many orders of magnitude (Kerridge et al. 1977).

Thus, the only convincing evidence to-date for nuclear reactions in the solar atmosphere are the gamma-ray line and neutron observations. The observed line energies and line ratios are fully consistent with nuclear reactions produced by particles of energies in excess of several MeV. As already mentioned, thermonuclear burning makes no measurable contribution to

these reactions. In Section II we review the interaction models for the production of gamma rays in energetic particle reactions and present new calculations of the production rates. In Section III we review the observational data on gamma-ray lines, we compare them with theory and we discuss their implications. Because the neutron observations are still very preliminary, we defer their analysis to future studies. We summarize our conclusion in Section IV.

II. NUCLEAR REACTIONS IN SOLAR FLARES

In this section we first summarize the formalism of the thin- and thick-target interaction models used in calculating nuclear reaction yields in solar flares, and we discuss the energetic particle spectra and compositions that we use in these calculations. We then evaluate, for the various models, the neutron and 2.223 MeV photon productions, the positron and 0.511 MeV photon productions and the productions of the various prompt nuclear deexcitation lines.

A. Interaction Models and Properties of the Energetic Particles

We consider first the thin-target model. Here nuclear reactions take place between accelerated particles and a cold ambient medium in an interaction volume from which particles escape with negligible energy loss and with an escape probability which is energy independent and the same for all types of particles. Let $N_j(E,t)dE$ be the instantaneous number of energetic particles of type j in the volume having energies per nucleon in dE around E, and n_i the density of ambient particles of type i. The instantaneous reaction rate between accelerated particles of type j and ambient particles of type i is given by

$$q_{ij}(t) = \int_o^\infty n_i \; N_j(E,t)\beta(E)\sigma_{ij}(E)dE \quad , \qquad (1)$$

where $\beta(E)$ is particle velocity and $\sigma_{ij}(E)$ is the energy dependent cross section of the reaction considered.

In the thin-target model the energetic particles that escape from the interaction region can, in principle, be observed in the interplanetary medium by detectors on spacecraft. The following relationship exists between the interplanetary particles, $N_{esc,j}(E)$, and the instantaneous number of particles in the thin-target interaction volume:

$$N_{esc,j}(E) = T^{-1} \int dt \; N_j(E,t) \; dt \quad . \qquad (2)$$

Here T is the escape time from the volume and the time integral is over the duration of the nuclear interactions. By integrating equation (1) over time, by substituting equation (2), and by summing over all i and j that contribute to a particular reaction product (e.g. neutrons, positrons, excited levels), we obtain the time-integrated nuclear reaction yield of that product in the thin-target model:

$$Q = n_H T \sum_{ij} (n_i/n_H) \int_o^\infty dE \; N_{esc,j}(E)\beta(E)\sigma_{ij}(E)dE \quad . \qquad (3)$$

As opposed to the thin-target model, in which the particles escape from the interaction region and can be observed in space, the thick-target model is one in which the particles produce nuclear reactions as they slow down in the solar atmosphere. In this model, the ambient density in the interaction region is expected to be quite high, (i.e. the region could be close to or

even inside the photosphere). Since particles, in general, are not accelerated in high density regions, it is reasonable to assume that in the thick-target model the acceleration takes place outside the interaction volume. Thus, let $\bar{N}_j(E)dE$ be the time-integrated number of particles of type j with E in dE incident on the interaction region. The time-integrated nuclear reaction yield can then be written as

$$Q = m_p^{-1} \sum_{ij} (n_i/n_H) \int_0^\infty \bar{N}_j(E)dE \int_0^E \sigma_{ij}(E') \left(\frac{dE'}{dx}\right)_j^{-1} dE' \quad , \qquad (4)$$

where m_p is the mass of the proton and $(dE/dx)_j$ is the energy loss rate per unit path length (measured in (MeV/nucleon)/(g/cm^2)) of accelerated particle j in the ambient solar atmosphere. In the present calculations we take $(dE/dx)_j$ equal to the energy loss rates of charged particles in a neutral medium,

$$\left(\frac{dE}{dx}\right)_j \approx \left(\frac{dE}{dx}\right)_{j,H} \left[1 + \frac{n_{He}}{n_H} \frac{m_{He}}{m_p} \frac{(dE/dx)_{j,He}}{(dE/dx)_{j,H}} \right] \quad . \qquad (5)$$

Here $(dE/dx)_{j,H}$ and $(dE/dx)_{j,He}$ are the energy loss rates of particle j in H and He, respectively, and m_{He} is the mass of ^{4}He. For the abundances of Table 1, the term in the square brackets is approximately 1.13 and essentially independent of energy. Using the tabulations of Barkas and Berger (1964) and Northcliffe and Schilling (1970), $(dE/dX)_{j,H}$ can be approximated by

$$\left(\frac{dE}{dX}\right)_{j,H} \approx (Z_{eff}^2/A)_j \quad 630 \; E^{-0.8} \text{(MeV/nucleon)/(g/cm}^2) \quad , \qquad (6)$$

where (Pierce and Blann 1968)

$$Z_{eff} = Z[\ 1 - \exp\ (-137\beta/Z^{2/3})] \quad , \tag{7}$$

and Z and A are the atomic and mass number of particle j. For computational purposes, it is convenient to invert the order of integration in equation (4),

$$Q = m_p^{-1} \sum_{ij} (n_i/n_H) \int_0^\infty dE\ \sigma_{ij}(E)\ (dE/dx)_j^{-1} \int_E^\infty dE'\ \bar{N}_j\ (E') \quad . \tag{8}$$

A detailed discussion of solar energetic particle spectra and compositions based on interplanetary observation are given in another article in this volume (Forman, Ramaty and Zweibel 1982). Various forms of accelerated particle spectra have been used in previous treatments of nuclear reactions in solar flares (Lingenfelter and Ramaty 1967, Ramaty, Kozlovsky and Lingenfelter 1975, Ramaty 1979). These are power laws in kinetic energy,

$$N_{esc,j}(E) \text{ or } \bar{N}_j\ (E) = \begin{cases} B_j E^{-S} & , \quad E > E_c \\ B_j E_c^{-S} & , \quad E \leq E_c \end{cases} \quad , \tag{9}$$

exponentials in rigidity,

$$N_{esc,j}(E) \text{ or } \bar{N}_j(E) = B_j \exp(\ -R_j/R_o)\ dR_j/dE \quad , \tag{10}$$

and Bessel functions,

$$N_{esc,j}(E) \text{ or } \bar{N}_j(E) = B_j K_2 \left[2(3p/(m_p c \alpha T))^{1/2} \right] \quad . \qquad (11)$$

In these expressions the B_j's are proportional to the abundances of energetic particles j, $R_j = (A/Z)_j p$ is particle rigidity, $p = \sqrt{E(E + 2m_p c^2)}$ is particle momentum per nucleon and K_2 is the modified Bessel function of order 2 (e.g. Abramovitz and Stegun 1966). The parameters s and E_c for power laws, R_0 for the exponential in rigidity, and αT for the Bessel function, characterize the spectrum of the energetic particles.

Recent observations of energetic protons and α-particles on spacecraft (McGuire, von Rosenvinge and McDonald 1981) indicate that power laws cannot fit the observed energy spectra of these particles. This result is consistent with earlier studies (Freier and Webber 1963) which have shown that exponentials in rigidity provide a better fit to the solar proton data than do power laws in kinetic energy. Therefore, we shall present new calculations of nuclear reaction yields only for the exponential spectrum of equation (10) and the Bessel function spectrum of equation (11). Calculations for power laws can be found in previous papers (Ramaty, Kozlovsky and Lingenfelter 1975, Ramaty, Kozlovsky and Suri 1977).

In Figure (1) we show the energy spectra of protons and α-particles observed by detectors on the IMP 8 spacecraft from the June 7,1980 flare (R. McGuire, private communication 1981). This flare is one of the best studied

gamma-ray flares observed by the SMM spectrometer (Chupp et al. 1981). As can be seen, the curves in Figure 1, given by $dj/dE \propto \beta K_2[2(3p/(m_p c(\alpha T))^{1/2}]$ with $\alpha T = 0.015$, provide a very good fit to the data. The June 7, 1980 flare is the only gamma-ray flare observed to-date for which good interplanetary energetic particle spectra have been reported. But even for this flare it is not entirely clear that all the interplanetary particles shown in Figure 1 were produced by the same flare as the one which produced the gamma-ray lines because of evidence for multiple injection of particles from the Sun (T. Von Rosenvinge, private communication 1981).

Equation (11) was shown (M. Lee private communication 1978, Ramaty 1979, Forman, Ramaty and Zweibel 1982) to be the solution of a Fokker-Planck equation for stochastic Fermi acceleration with acceleration efficiency coefficient, α, and escape time, T, which are independent of particle energy and particle charge. While there is no guarantee that such a simple acceleration model is appropriate for solar flares, we feel that the spectrum of equation (11) can be adequately used for the analysis of the presently available gamma-ray data, particularly since this spectrum also provides a good fit to the observed interplanetary particle energy spectra, as can be seen from Figure 1 and from the more detailed analysis of McGuire, von Rosenvinge and McDonald (1981).

The particle abundances that we use in the present calculation are given in Table 1. The ambient medium abundances (Cameron 1981) are listed in the second column. From interplanetary observations, it is well known that the energetic particle abundances vary substantially from one flare to another (e.g. Forman, Ramaty and Zweibel 1982). In the present calculations we use two sets of energetic particle abundances. The first set, denoted by EP1, is given in the third column of Table 1, and the second set, EP2, is identical to

the ambient medium abundances of the second column. The energetic particles EP1 are significantly richer in heavy elements than EP2.

B. Neutron and 2.223 MeV Photon Production

The strongest line observed in nearly all gamma ray flares is that at 2.223 MeV from neutron capture on hydrogen, $^1H(n,\gamma)^2H$. Several theoretical studies have been made of neutron production in solar flares (Lingenfelter et al. 1965, Lingenfelter and Ramaty 1967, Ramaty, Kozlovsky and Lingenfelter 1975) and of 2.223 MeV photon production from the capture of these neutrons in the solar atmosphere (Wang and Ramaty 1974, Kanbach et al. 1975). The neutron production cross sections have been discussed in considerable detail by Ramaty, Kozlovsky and Lingenfelter (1975). These cross sections have recently been updated (B. Kozlovsky and R. E. Lingenfelter, private communication 1981) with the addition of many new reactions that involve all the isotopes listed in Table 1. These new cross sections, to be published elsewhere, are used in the present calculations.

The calculated neutron production yields, Q_n, in the thin and thick-target models are shown in Figure 2. These calculations are normalized such that the number of escaping protons of energies greater than 30 MeV, $N_{esc,p}(>30\ MeV)$, and the number of protons incident on the thick target above the same energy, $\bar{N}_p$ (>30 MeV), are both equal to unity. The energetic particles abundances are given by EP1 (see Table 1). For relatively flat energetic particle spectra, corresponding to large values of R_0 or αT, the bulk of the neutrons are produced in reactions between protons and α-particles. For steep particle spectra, given by the Bessel function at small αT, the large neutron yields result from reactions between α-particles and heavy nuclei. These large neutron yields are absent for the rigidity

spectra because particles with $Z \geq 2$ have lower energies per nucleon at the same rigidity and hence produce less nuclear reactions. These effects were discussed in more detail by Ramaty, Kozlovsky and Lingenfelter (1975) in connection with the camparison of neutron production by particles with spectra that were either power laws in energy or exponentials in rigidity.

In Figure 3 we show partial neutron production rates in the thick target model for energetic particle spectra given by equation (11) and abundances again given by EP1. The curves labelled p, α, CNO and Ne-Fe represent, respectively, neutron yields of energetic protons, α-particles, C, N and O nuclei, and nuclei from Ne through Fe interacting with the ambient solar atmosphere. As can be seen, except for the very steep particle spectra (small αT) the neutrons result mostly from α-particles and protons. For very flat spectra, the neutron yield of protons includes an important contribution from the reaction $p+p \rightarrow p+n+\pi^+$.

In Figure 4 we show the energy in accelerated particles required to produce one neutron in the thick-target model. Here W is defined by

$$W = \sum_j A_j \int_E^\infty dE' \, E' \, \bar{N}_j(E') \quad , \tag{12}$$

where $\bar{N}_j(E)$ is given by equation (11) and the abundances are given by EP1. As can be seen from Figure 4, for $\alpha T = 0.015$, appropriate for the June 7, 1980 flare (see Figure 1), more than $1/2$ of the accelerated particle energy is contained in particles of energies greater than 1 MeV/nucleon and this fraction increases with increasing αT. A much lower fraction of the energy content, however, resides in particles of higher energies.

The values of W/Q_n given in Figure 4 should be considered as lower limits because the particle energy loss rate (equation 6) is valid only for slowing down of test particles in a neutral medium. In a fully ionized medium, the slowing-down rate of test particles is larger by about a factor of 3(e.g. Ramaty 1979). Furthermore, collective effects, such as the generation of an induced magnetic field by a beam of particles (Hoyng, Brown and Van Beek 1976, Colgate 1978) would increase the energy required for the production of a given amount of neutrons.

The 2.223 MeV gamma-ray line is formed by neutron capture on ^1H in the photosphere. To study this line formation, Wang and Ramaty (1974) have carried out a detailed Monte-Carlo simulation in which a distribution of neutrons was released above the photosphere, and the path of each neutron after its release was followed. For isotropic neutron release, any initially upward moving neutron escapes from the Sun. Some of the downward moving neutrons can also escape after being backscattered elastically by ambient protons, but most of these neutrons either are captured or decay at the Sun. Because the probability for elastic scattering is much larger than the capture probability, the majority of the neutrons are thermalized before they get captured. Since the thermal speed in the photosphere (where most of the captures take place) is very much smaller than the speed of light, the energy of the gamma rays is almost exactly 2.223 MeV (Taylor, Neff and King 1967), and the Doppler-broadened width of the line is very small ($\lesssim$100 eV) (Ramaty, Kozlovsky and Lingenfelter 1975). The energy of the line observed with the high resolution Ge detector on board HEAO-3 from the November 9, 1979 flare is 2.225 ± 0.002 MeV (Prince et al. 1982).

The bulk of neutrons at the Sun are captured either on ^1H or on ^3He. Whereas capture on ^1H yields a 2.223 MeV photon, capture on ^3He proceeds via

the radiationless reaction $^3He(n,p)^3H$ and hence produces no photons. The cross sections for capture on ^1H and ^3He are $2.2\times10^{-30}\ \beta_n^{-1}\ cm^2$ and $3.7\times10^{-26}\ \beta_n^{-1} cm^2$, respectively, where $c\beta_n$ is the velocity of the neutron (for details see Wang and Ramaty 1974). Thus, if the $^3He/H$ ratio in the photosphere is $\sim 5\times10^{-5}$, comparable to that observed in the solar wind (Geiss and Reeves 1972) and in the chromosphere (Hall 1975), nearly equal numbers of neutrons are captured on ^3He as on H.

The results of the Monte-Carlo calculations of Wang and Ramaty (1974) are presented in Figure 5. In these calculations an isotropic distribution of monoenergetic neutrons of energy E_n is released above the photosphere. The solid lines are the probabilities for the various indicated processes. As can be seen, the capture and loss probabilities increase with increasing energy, because higher energy neutrons penetrate deeper into the photosphere. This reduces their escape probability and leads to a shorter capture time, thereby reducing the decay probability. The probability for loss on ^3He almost equals the capture probability on protons. The escape probability is greater than 0.5, because all initially upward moving neutrons were assumed to escape from the Sun. Note that the sum of all probabilities equals 1.

The dashed curves in Figure 5, are neutron-to-photon conversion coefficients evaluated (Wang and Ramaty 1974) for specific emission angles θ between the Earth-Sun line and the vertical to the photosphere and given neutron energies. At low neutron energies and θ near zero, $f_{2.2}$ is close to the capture probability on protons. This means that gamma rays from low-energy neutrons observed close to the vertical escape essentially unattenuated from the Sun. At higher energies and at larger angles, however, there is significant attenuation of the gamma rays due to Compton scattering in the photosphere. Therefore, for flares close to the limb of the Sun, the 2.223

MeV line should be strongly attenuated in comparison with other nuclear deexcitation lines which are likely to be produced at higher altitudes in the solar atmosphere than the 2.223 MeV line. As we shall see in Section III A, this limb darkening is clearly seen in the SMM data.

The time integrated flux, or fluence, of 2.223 MeV photons at Earth resulting from neutron capture at the Sun can be written as

$$\phi(2.223\ \text{MeV}) = Q_n \bar{f}_{2.2}/(4\pi d^2) \quad , \qquad (13)$$

where d = 1 AU and $\bar{f}_{2.2}$ is the neutron-to-2.223 MeV photon conversion coefficient averaged over the neutron energy spectrum. For $\theta = 0$, Ramaty, Kozlovsky and Lingenfelter (1975) find that $\bar{f}_{2.2}$ ranges from about 0.1 to 0.14, depending on the neutron energy spectrum. However, in the thick-target model, the neutron angular distribution is probably not isotropic and the neutrons could be produced in the photosphere (Kanbach et al. 1975). These effects should increase $\bar{f}_n$ by as much as a factor of 2. In our subsequent discussion we denote by the conversion coefficient for vertical escape by $\bar{f}_{2.2}(0)$. The SMM calculations now definitely justify new and more accurate calculations of neutron capture in the photosphere. These have not yet been carried out. Nevertheless, using the presently available calculations, we believe that $\bar{f}_{2.2}(0)$ should not exceed 0.3.

C. Positron and 0.511 MeV Photon Production

The 0.511 MeV gamma-ray line resulting from positron annihilation has been observed from several solar flares. Positrons in flares are produced in energetic particles interaction with the ambient solar atmosphere. A number of theoretical studies have been made of positron production in such

interactions (Lingenfelter and Ramaty 1967, Ramaty, Kozlovsky and Lingenfelter 1975) and the positron slowing down and annihilation (Crannell et al. 1976, Bussard, Ramaty and Drachman 1979). In the present paper we give the results of new calculations (B. Kozlovsky and R. E. Lingenfelter, private communication 1981) of positron production based on a large number of β^+ emitters produced in nuclear reactions that involve all the isotopes listed in Table 1. The results are given in Figure 6, where we show the ratio Q_+/Q_n for the thin- and thick-target models. Here Q_+ is calculated from equations (3) and (8), respectively, with energetic particles given by equation (11). The positron yields shown in this figure represent total yields. Because of the finite half-lives of the various β^+ emitters, however, in a short observation time of a transient event, fewer positrons than indicated in Figure 6 are available for 0.511 MeV line production. This effect is shown in Figure 7, where dQ_+/dt is the instantaneous production rate of positrons from a burst (δ-function in time) of β^+-emitters produced at $t = 0$.

The positrons produced in nuclear reactions have initial energies ranging from about 0.1 MeV to tens of MeV, depending on the production mode. In a thick-target, these positrons are rapidly slowed down to energies of tens of eV where the majority of them form positronium atoms. The slowing down time, t_s, plus the positronium formation time, t_{pos}, are shown in Figure 8 as a function of initial positron energy for an ambient medium of temperature 10^4K, degree of ionization η and ambient density 10^{11} cm^{-3} and 10^{13} cm^{-3} (from calculations of J. M. McKinley, private communication 1981). The dependence of $(t_s + t_{pos})^{-1}$ on density is essentially linear.

The annihilation of positronium atoms is quite rapid (Heitler 1954). If formed in the singlet state (25% of the time), positronium annihilates at a rate of 8×10^9 sec^{-1} into two 0.511 MeV gamma rays. In the triplet state

(formed 75% of the time) it annihilates at a rate of 7×10^6 sec^{-1} into three photons of energies less than 0.511 MeV. This 3-photon continuum is, in principle, observable if the density of the ambient medium is less than $\sim 10^{15}$ cm^{-3}. At a higher density collisions break up triplet positronium before it can annihilate (Crannell et al. 1976).

We define a positron-to-0.511 MeV photon conversion coefficient, $\bar{f}_{0.51}$ analogous to $\bar{f}_{2.2}$ discussed above, such that the time integrated flux, or fluence, of 0.511 MeV photons at Earth resulting from positron emitter production at the Sun is given by

$$\phi(0.511 \text{ MeV}) = Q_+ \bar{f}_{0.51}/(4\pi d^2) \quad . \qquad (14)$$

Various effects influence the value of $\bar{f}_{0.51}$. If all the β^+ emitters produced in the flare decay during the observation period and if all the resultant positrons annihilate in this period, then $\bar{f}_{0.51}$ ranges from 0.5 to 2, depending on the fraction of positrons that annihilate via positronium. But if the observation period is shorter than the decay halflives of the dominant β^+ emitters, or if some of the positrons escape from the Sun into low density regions where their annihilation time is long, $\bar{f}_{0.51}$ can be substantially lower than the above values. For limb flares, there may be significant Compton scattering of the 0.511 MeV photons in the photosphere if the nuclear reactions themselves take place in the photosphere. This will also lower the value of $\bar{f}_{0.51}$.

Another observable of considerable interest is the width of the 0.511 MeV line. The dependence of this width on temperature, degree of ionization and density was studied in considerable detail by Crannell et al. (1976) and Bussard, Ramaty and Drachman (1979). Using their results, we find that the

0.511 MeV line should be narrower than about 3.5 keV if the temperature of the annihilation site is less than 10^5K. At higher temperatures the width should vary as $T^{1/2}$, with a full width at half maximum of about 11 keV at 10^6K.

D. Prompt Deexcitation Line Production

A variety of gamma-ray lines are produced in solar flares from de-excitation of nuclear levels. Figure 9 shows the spectrum from these de-excitations, calculated (Ramaty, Kozlovsky and Lingenfelter 1979) by employing a Monte-Carlo simulation for an energetic particle population interacting with an ambient medium. The energetic particle spectrum is proportional to E^{-2} (equation 9 with $E_c = 0$) and both the ambient medium and the energetic particles at the same E have a photospheric composition. The shapes of the lines are evaluated by taking into account nuclear kinematics and data on the differential cross-sections of the reactions. The results of the simulations are binned into energy intervals ranging from 2 to 5 keV (as indicated in the figure), consistent with the resolution of a Ge gamma-ray spectrometer.

Two line components can be distinguished in Figure 9. A narrow component resulting from the deexcitation of ambient, heavy nuclei excited by energetic protons and α-particles, and a broad component from the deexcitation of energetic heavy nuclei interacting with ambient H and He. The nuclei responsible for the emission of the strongest narrow lines are indicated in the figure.

In addition to these strong narrow lines, there are many other weaker narrow lines, which together with the broad component produced by heavy accelerated particles, merge into the underlying continuum. Above ~ 4 MeV most of the radiation is from C, N, and O, while below about 3 MeV the

principal contributors are Mg, Si and Fe. It has been shown (Ramaty, Kozlovsky and Suri 1977, Ibragimov and Kocharov 1977) that the bulk of the gamma-ray flux observed between 4 and 7 MeV from the August 4, 1972 flare was of such nuclear origin rather than electron bremsstrahlung or other continuum emission processes. In addition, a substantial fraction of the photons in the 1 to 2 MeV band could be nuclear radiation resulting from an enhanced abundance of Ne, Mg, Si and Fe in the energetic particles (Ramaty et al. 1980 and Section III A). The 4 to 7 MeV energy band, referred to in the SMM observations as the "main channel window", can provide a direct and sensitive measure of the interaction rate of protons and nuclei in solar flares (Section III A, B).

Because the cross sections for excitation of nuclear levels have different energy dependences from those of neutron and positron production, the calculated ratios of nuclear deexcitation line yields to the neutron yield depend strongly on the assumed spectra of the accelerated particles and on the interaction model. As an example, in Figure 10 we show the ratio $Q(4.44)/Q_n$ for the two interaction models as a function of αT for the Bessel function spectrum of equation (11). Here $Q(4.44)$ is the yield of the narrow 4.44 MeV line calculated from equations (3) or (8), for thin or thick targets, respectively, with energetic particle abundances given by EP1 (see Table 1). As can be seen, $Q(4.44)/Q_n$ generally decreases with increasing energetic particle spectral hardness, reflecting an increased neutron production and decreased 4.44 MeV photon production by particles of high energies. Likewise, this ratio is lower for thick targets than for thin targets (except for very steep particle spectra) because the energy losses harden the particle spectra in the thick target. For very steep (small αT) Bessel function spectra, the thick-target ratio exceeds that for thin targets. This results from the

effect of the energy losses in the thick-target which suppress the heavy particle fluxes relative to the proton and α-particle fluxes. At low particle energies, the heavy particles contribute significantly to neutron production but not to the production of narrow 4.44 MeV photons.

As already mentioned, the photon energy band from 4 to 7 MeV is an important measure of the interaction rate of protons and nuclei in solar flares. In Figure 11 we show the ratio of the photon yield in this band, Q(4-7), to the neutron yield Q_n. Here Q(4-7) is calculated from equations (3) or (8) for thin or thick-targets, respectively, together with a Monte-Carlo simulation similar to that employed in the evaluation of the gamma-ray spectrum of Figure 9. In this calculation we use both the EP1 and EP2 energetic particle abundances.

The same trends as in Figure 10 are also evident for $Q(4-7)/Q_n$ in Figure 11. $Q(4-7)/Q_n$ decreases with increasing αT and is larger in the thick-target than in the thin-target model. The variation of $Q(4-7)/Q_n$ with energetic particle composition, however, is not very large, because several particle species contribute simultaneously to both Q(4-7) and Q_n.

The ratio Q(4.44)/Q(4-7) is shown in Figure 12 for thin and thick targets and the energetic particle abundances EP1 and EP2. As can be seen, this ratio does not depend strongly on energetic particle spectrum because of the similar energy dependences of all prompt line production cross sections. However, Q(4.44)/Q(4-7) is smaller for the thin target than for the thick target, because for the latter the contribution of the heavy particles is suppressed by the energy losses. Likewise Q(4.44)/Q(4-7) is lower for EP1 than for EP2 because the former contains more heavy particles relative to protons than does the latter.

The shapes and peak energies of prompt nuclear gamma-ray lines are

sensitive to anisotropies in the energetic particle angular distributions. Thus, Ramaty and Crannell (1976) have evaluated the shift in the peak of the 6.129 MeV lines resulting from energetic particle beaming, while Ramaty, Kozlovsky and Lingenfelter (1979) discussed the splitting of 4.438 MeV line that is observed (Kolata, Auble and Galonsky 1967) when the excited ^{12}C nuclei are produced by a proton beam perpendicular to the direction of observation.

A unique test of energetic particle beaming was proposed by Kozlovsky and Ramaty (1977). This concerns the $^{7}Be^{*}$ and $^{7}Li^{*}$ deexcitation lines at 0.431 and 0.478 MeV produced in the reactions $^{4}He(\alpha,n)^{7}Be^{*}$ and $^{4}He(\alpha,p)^{7}Li^{*}$, respectively. Here the stars indicate nuclei in excited states. The shapes of these lines are shown in Figure 13. As can be seen, if the angular distribution of the energetic α-particles is isotropic, the Doppler broadening of the two lines is so large that they blend into a single feature that cannot, in general, be observed in the presence of a strong continuum. If, however, the α-particles are beamed, the line widths are much less than in the isotropic case and two discrete lines can be seen. In particular, if the direction of observations is perpendicular to the beam (as in Figure 13) the lines appear close to the rest energies of 0.431 MeV and 0.478 MeV.

The fluence at Earth in the 4-7 MeV channel is given by

$$\phi(4\text{-}7\ \text{MeV}) = Q(4\text{-}7\ \text{MeV})\ \bar{f}_{4-7}/(4\pi d^2) \quad , \tag{15}$$

where $\bar{f}_{4-7}$ is the conversion coefficient from nuclear deexcitations to photons observed. If the excited nuclei are produced isotropically and if there is no attenuation of the photons, $\bar{f}_{4-7} = 1$. However, if the protons and nuclei form a beam pointing away from the observer, then from the Monte-Carlo calculations described above we find that $\bar{f}_{4-7} \approx 0.8$. Thus,

provided that there is not much attenuation, we expect that $0.8 \lesssim F_{4-7} \lesssim 1$, depending on the geometry of the interacting particles.

III. IMPLICATIONS OF GAMMA RAY OBSERVATIONS

In this Section we consider the implications of the gamma-ray line observations on the nature of the interaction model (thin- or thick-target), on the accelerated particle spectrum, on the energy deposited by the particles and the number of particles that interact to produce the gamma rays, on the timing of the acceleration, on the photospheric ^{3}He abundance, and on the beaming of the energetic particles.

The solar flares with observed gamma-ray lines are listed in Table 2. The August 4 and August 7, 1972 events were observed by Chupp et al. (1973) with the spectrometer on board OSO-7. The data given in Table 2 for the August 4, 1972 flare is from Chupp (1976), except for ϕ(4-7 MeV) which is from the analysis of Ramaty, Kozlovsky and Suri (1977). We have multiplied the time averaged fluxes given in these references by 553 sec, the observation time of gamma rays from this flare (Chupp 1976). Because of Earth occultation of the orbiting gamma-ray detector, however, the total duration of gamma-ray emission from the August 4 flare was longer than this time interval. From the analysis of Wang and Ramaty (1975), we estimate that all fluences in Table 2 for the August 4 flare should be increased by about a factor of 2, but without a significant modification of $\phi(4\text{-}7)/\phi(2.22)$.

Only the 2.22 and 0.51 MeV lines were observed from the August 7, 1972 event (Chupp 1976) because the detector was behind the Earth during the flash phase of the flare. These observations clearly demonstrate the delayed nature of these two lines: at a time when all prompt emissions were very small, the 2.22 and 0.51 MeV lines were still observable.

The data for the flares of July 11, 1978 and November 9, 1979 are, respectively, from Hudson et al. (1980) and (Prince et al. 1982).

The data for the other flares listed in Table 2, still believed to be preliminary, were observed with the gamma-ray spectrometer on SMM (Chupp 1982). Because of the very high intensity of the June 21, 1980 flare, the SMM detector saturated during the flash phase of this event. Delayed 2.22 and 0.51 MeV lines, as well as high energy neutrons (Chupp and Forrest 1981), were observed from the June 21 flare.

The ratios of the photon fluence in the 4 to 7 MeV channel to that in the 2.22 MeV line, shown in Table 2, follow directly from the data except for the July 11, 1978 flare where $\phi(4\text{-}7)$ is determined using a theoretical ratio $Q(4.44)/Q(4\text{-}7) \simeq 0.25$. The fact that this ratio is model dependent (Figure 12) leads to some uncertainty in the determination of $\phi(4\text{-}7)$ for this flare.

A. Interaction Model, Energetic Particle Spectrum, Number and Energy Content

We first consider the flare of June 7, 1980 for which there are both gamma-ray line observations and interplanetary particle measurements. The combined analysis of these data imply that for this flare the bulk of the gamma-ray line emission results from thick target interactions. Furthermore, most of the energetic protons and nuclei that produce the gamma-ray lines remain trapped in the solar atmosphere and only a small fraction of them escapes into the interplanetary medium.

The location of the June 7 flare at N12W74 indicates that it was well connected magnetically (e.g. Van Hollebeke, Ma Sung and McDonald 1975), so that particles escaping from the Sun could be observed in interplanetary space near the orbit of the Earth. Indeed, several observations of energetic particles have been reported (von Rosenvinge, Ramaty and Reames 1981, Evenson,

Meyer and Yanagita 1981, Pesses et al. 1981). Based on those, the number of protons of energies greater than 10 MeV released into the interplanetary medium, $N_{esc,p}(>10\ MeV)$, has been estimated (von Rosenvinge et al. 1981) to be $\sim 10^{31}$. As can be seen from Figure 1, the spectrum of these protons is well fit with the Bessel function of equation (11) with αT equal to 0.015 (R. McGuire, private communication 1981). This spectral form also fits the α-particle spectrum with essentially the same αT. For $\alpha T = 0.015$, $N_{esc,p}(>10$ MeV) $\approx 10^{31}$ implies $N_{esc,p}(>30\ MeV) \approx 5\times10^{29}$. If the gamma rays were produced by thin-target interactions, then from equation 3, with the numerical results of Figure 2 and $\bar{f}_{2.2} = 0.12$ (appropriate for a thin target), the observed 2.22 MeV line fluence (Table 2) implies that $n_H T \approx 7.4\times10^{14}$ $cm^3 sec^{-1}$. This is equivalent to a matter traversal for 30 MeV/nucleon particles of $\approx 13 g/cm^2$. The large abundances of spallation products (^2H, ^3H, Li, Be, B) that would result from such a long path length are not observed from solar flares (e.g. McGuire, von Rosenvinge and McDonald 1977). This indicates that the gamma-ray lines observed from the June 7,1980 flare were probably not produced in thin-target interactions. In the thick-target models, on the other hand, the spallation products that accompany the production of gamma-ray lines, are slowed down in the solar atmosphere and hence are not expected to be seen in the interplanetary medium.

Analysis of the ratio of the 4 to 7 MeV fluence to the 2.223 MeV line fluence for the June 7, 1980 flare also suggests that the observed gamma rays were produced in thick-target interactions, not thin-target. This can be seen as follows:

From equations 13 and 15, with $\bar{f}_{4-7} = 1$, the neutron-to-2.223 MeV photon conversion coefficient, $\bar{f}_{2.2}$, can be written as

$$\bar{f}_{2.2} = \frac{Q(4\text{-}7\ \text{MeV})/Q_n}{\phi(4\text{-}7\ \text{MeV})/\phi(2.22\ \text{MeV})} \quad . \qquad (16)$$

The numerator can be obtained from theory (see Figure 11) if αT is known. The interplanetary particle data suggests that $\alpha T \simeq 0.015$ (Figure 1) provided that all the observed particles were indeed produced in the gamma-ray flare and that the flare particle spectrum is not greatly modified by the escape process and interplanetary propagation. The denominator in equation (16) is from the gamma-ray data, $\phi(4\text{-}7)/\phi(2.22) \simeq 1.74$ (Table 2). Then for thin target interactions, $Q(4\text{-}7)/Q_n \simeq 0.7$, hence $\bar{f}_{2.2} \simeq 0.4$, while for thick target interactions, $Q(4\text{-}7)/Q_n \simeq 0.25$ hence $\bar{f}_{2.2} \simeq 0.14$. From the calculations of Wang and Ramaty (1974) and Kanbach et al. (1981) we estimate that for the location of the June 7, 1980 flare, $\bar{f}_{2.2}/\bar{f}_{2.2}(0) \simeq 0.6$. For this flare, therefore, $\bar{f}_{2.2}(0)$ would have to be ~ 0.67, if the gamma rays were made in thin-target interactions, and ~ 0.23 if they were made in thick-target ones. The former value is clearly inconsistent with the range of values of $\bar{f}_{2.2}(0)$ obtained from the Monte-Carlo simulations of neutron production in the solar atmosphere (Section II B). The latter value, for the thick target, is quite consistent with these calculations provided the neutrons are produced in the photosphere and/or their initial angular distribution is skewed downwards toward the photosphere.

We proceed now to analyze the rest of the data listed in Table 2. We note the relatively small variability of $\phi(4\text{-}7)/\phi(2.22)$ from one flare to another. The exception is the limb flare of April 27, 1981 for which the 2.22 MeV line is strongly attenuated by Compton scattering as the photons emerge from the photosphere at large angles to the local normal (Wang and Ramaty 1974). We assume that in all of these flares, as in the June 7 flare, the gamma rays are produced by thick-target interactions. This is justified

because different interaction models for different flares would not be consistent with the relative constancy of $\phi(4\text{-}7)/\phi(2.22)$ shown in Table 2. Furthermore, we assume the same neutron-to-2.223 photon conversion coefficient for all flares, except for the correction due to flare location. We use $\bar{f}_{2.2}(0) = 0.23$, a value consistent with both theory and the June 7 particle and gamma-ray data.

Table 3 lists the flares with available $\phi(4\text{-}7)/\phi(2.22)$ ratios and the April 27, 1981 flare. The second column gives an estimate of $\bar{f}_{2.2}/\bar{f}_{2.2}(0)$ obtained from the flare locations and the calculations of Wang and Ramaty (1974) and Kanbach et al. (1981). The third column lists values of $Q(4\text{-}7)/Q_n$ deduced from equation (16), while the fourth column provides the value of αT obtained from these ratios and Figure 11. We note the relatively small variability of αT from one flare to another, a direct consequence of the constancy of $\phi(4\text{-}7)/\phi(2.22)$. This result is consistent with the observations of McGuire, von Rosenvinge and McDonald (1981) who find a range of αT's for protons and α-particles in interplanetary space which essentially overlaps that deduced for the gamma-ray flares. Particle acceleration evidently produces energy spectra that do not vary much from flare to flare. A similar conclusion has been obtained by Van Hollebeke, Ma Sung and McDonald (1975).

We cannot deduce the αT for the limb flare of April 27, 1981 because of the strong attenuation of the 2.223 MeV line by Compton scattering in the photosphere. The small variability of αT, however, allows us to assume an αT for this flare. We take $\alpha T = 0.019$, equal to that for the August 4, 1972 flare, because both events have similar durations of gamma-ray emission and approximately equal fluences in the 4 to 7 MeV channel.

Using the αT's listed in column 4, we calculate, in the thick-target model, the number of particles that interact in the solar atmosphere and the

energy deposited by them. The results, based on the numerical values of Figures 2 and 4 are given in columns 5 and 6 of Table 3. Here, W(>1 MeV/nucleon) is the energy deposited by particles of energies greater than 1 MeV/nucleon and $\bar{N}_p$(>10 MeV) is the number of protons of energies greater than 10 MeV incident on the thick-target. For the June 7, 1980 flare, the number of protons of energies greater than 10 MeV that interacts at the Sun exceeds that observed in interplanetary space ($\sim 10^{31}$) by about two orders of magnitude. In contrast, for the August 4, 1972 flare, the number of protons above 10 MeV observed in the interplanetary medium ($\sim 3 \times 10^{35}$, Lin and Hudson 1976) exceeds the number that interacts at the Sun (Table 3) by more than an order of magnitude.

The very large number of interplanetary particles observed from the August 4, 1972 flare could have produced the observed gamma rays by thin-target interactions, as proposed by Lin and Hudson (1976). These authors have assumed a flatter energetic particle spectrum than that given by αT = 0.019 in Table 3. However, the interplanetary particle spectrum from the August 4 flare is only very poorly known because several interplanetary shocks were present at that time. Rather than using the interplanetary observations, we would now argue that the relative constancy of $\phi(4\text{-}7)/\phi(2.22)$ supports the same interaction model for all gamma-ray flares, and hence a thick-target model for the August 4, 1972 flare. This result is consistent with the average interplanetary proton spectrum observed (Webber et al. 1975) from August 2 to 11, which can be well fitted with equation (11) with αT = 0.02, in good agreement with the value of αT given in Table 3 for a thick-target.

The energy depositions of the protons and nuclei given in Table 3 range from about 5×10^{28} erg to 2.5×10^{30} erg. However, as pointed out in Section II B, these should be considered as lower limits only, because of additional

energy losses to the ionized component of the solar atmosphere and possible collective effects (e.g. Colgate 1978). Nevertheless, we can compare the energy deposition of the nucleonic component with that of >25 keV electrons deduced from hard X-ray observations in a nonthermal model (Lin and Hudson 1976). The energy deposition of the electrons ranges from about 2×10^{29} erg for small flares to $\sim 10^{32}$ ergs for the August 4, 1972 flare (Lin and Hudson 1976). We see that the nucleonic component could be responsible for the deposition of at least several percent of the total flare energy.

A final argument that supports the thick-target interaction model comes from the analysis of the 0.511 MeV line from positron annihilation. In Table 4 we list four flares for which there is either an observation of, or an upper limit on the fluence in this line. For the August 4, 1972 flare the data is from Chupp (1976), for the June 7 and July 1, 1980 flares it is from Chupp (1982) and for the April 27, 1981 flare it is from D. Forrest (private communication 1981). Using the αT's of Table 3 and the results of Figures 6 and 11, we calculate the ratios $Q_+/Q(4\text{-}7\ \text{MeV})$. These are shown in column 4 of Table 4. In column 5 of this table we give the values of $\phi(0.51)$ calculated from the values of $\phi(4\text{-}7\ \text{MeV})$ given in Table 2 and with $\bar{f}_{0.51}$, the β^+ emitter-to-0.511 MeV photon conversion coefficient, a free parameter. The observed fluences or upper limits are given in column 6. By comparing the calculated and observed values of $\phi(0.51)$, we see that for the August 4 event there is good agreement if $\bar{f}_{0.51}$ is about 0.7 which is consistent with the theoretical expectation discussed in Section II C. A similar value of $\bar{f}_{0.51}$ could also account for the July 1, 1980 data. For the June 7, 1980 flare, $\bar{f}_{0.51}$ would have to be less than about 0.4, a value consistent with the short observation period (50 sec) which does not allow the complete decay of all the positron emitters produced by the nuclear reactions (see Figure

7). To account for the observed upper limit, the value of $\bar{f}_{0.51}$ for the April 27, 1981 flare, however, must be less than about 0.2 even though the observation period here (~ 2000 sec) is sufficiently long for the decay of essentially all of the positron emitters. It appears that the best explanation of the absence of the 0.511 MeV line in the April 27,1981 limb flare is Compton scattering in the photosphere (Ramaty, Lingenfelter and Kozlovsky 1982). Because the neutrons have relatively long stopping ranges, Compton scattering of the 2.22 MeV line in limb flares is expected whether or not the nuclear reactions take place in the photosphere. But because the positrons have generally shorter ranges, the 0.511 MeV line will be Compton scattered in such flares only if the nuclear reactions themselves take place in the photosphere. This result, if substantiated by further studies, should be a strong argument for the validity of the thick-target model.

B. Time Dependences

The time dependences of the gamma-ray lines contain important information on a variety of questions in solar physics.

The time dependence of the strongest discrete line from flares, the 2.223 MeV line from neutron capture, is determined by the time history of the neutron production as well as by the removal rate of neutrons from the photosphere where they spend most of their time (~1 minute) between production and radiative capture (Section II B).

The delay between neutron production and 2.223 MeV photon release has been unmistakably observed in several flares (Chupp et al. 1973, Hudson et al. 1980, Chupp et al. 1981, Prince et al. 1982). Such an observation entails the comparison of the time history of a prompt photon flux, for example that in the 4 to 7 MeV channel, with that of the 2.223 MeV line. This has been

carried out in detail for the June 7, 1980 flare (Chupp et al. 1981). According to Chupp (1982), the characteristic neutron removal time from the photosphere, as deduced from the gamma-ray data, is on the order 50 seconds, consistent with theory (Section II B) and a photospheric $^3He/H$ ratio of $\sim 5 \times 10^{-5}$. As we shall see below (Section IIIC), the fact that the delay between neutron production and capture is not much shorter than 50 sec can place an upper limit on the photospheric ^3He abundance.

The time dependence of the 0.511 MeV line is determined by the production rate of the β^+ emitters, the decay rate of these emitters (Figure 7) and the slowing down and annihilation time of the positrons (Figure 8). Considerable information on the annihilation site of the positrons should become available from the comparison of observable time dependences of the 0.511 MeV line with theory. No such comparison has yet been done with the SMM data.

Because of the delayed nature of both the 2.223 and 0.511 MeV lines, information on the timing of the acceleration of protons and nuclei can be best obtained from prompt nuclear deexcitation lines. The comparison of the time histories of such lines with those of hard X-rays of various energies can give information on the possible existence of multiple acceleration stages of energetic particles in solar flares. Because the 4 to 7 MeV channel is dominated by nuclear radiation (Section III A), the flux in this channel (the "main channel window" in the SMM data) is an excellent diagnostic of the timing of acceleration of the nucleonic component in flares.

The time history of the "main channel" flux was observed for the June 7, 1980 flare (Chupp 1982). In particular, several gamma-ray spikes were seen in good correlation with the seven hard X-ray spikes (Kiplinger et al. 1982). From the comparison of these two time histories it follows that, at least for the June 7 flare, the <100 keV electrons and >10 MeV nuclei were accelerated

in very close time proximity (less than a few seconds). There is, nevertheless, a delay of approximately 2 sec between the hard X-ray and gamma-ray peaks. Bai (1982) suggests that this delay is due to two-step acceleration, where the first step accelerates the <100 keV electrons and the second step accelerates the mildly relativistic electrons and the nuclei (see also Bai and Ramaty 1979). On the other hand, Chupp (1982) attributes the delay to the difference in propagation time of $\geq$10 MeV/nucleon nuclei and $\leq$100 keV electrons along a magnetic arch of length $\sim 10^{10}$cm. In any case, the rapid decay ($\sim$ 2 seconds) of the main channel emission for the June 7, 1980 flare requires a sufficiently high ambient density ($>10^{13}$cm^{-3}) and this provides additional support for the validity of the thick-target model for this flare.

The time dependences of the various hard photon emissions for the June 7, 1980 flare were quite different from those of the longer duration August 4, 1972 flare. For the latter, the X-ray continuum above 350 keV reached peak strength a few minutes later than the continuum above 30 keV and the 2.22 MeV line profile was better explained when the neutron-production time profile was assumed to be similar to the time profile of the >350 keV continuum rather than the <100 keV continuum (Bai and Ramaty 1976, Bai 1982). These results, together with earlier X-ray observations (Frost and Dennis 1971) and gamma-ray measurements (Hudson et al. 1980, Willet et al. 1982) demonstrate that not all energetic particle populations in flares are accelerated at the same time. The present status of the existence of multiple acceleration phases in flares has been reviewed by Bai (1982).

C. The Photospheric ^{3}He Abundance

The abundance of ^{3}He in the solar atmosphere is of considerable astrophysical interest. Along with ^{2}H and ^{4}He, ^{3}He is formed by nucleosynthesis in the big bang (Wagoner 1973). In addition, stellar evolution should increase the ^{3}He abundance. In particular, the Sun should have burned into ^{3}He any amount of deuterium it originally had but the ^{3}He should not have been further burned into ^{4}He (Geiss and Reeves 1972 and references therein). Thus, a measurement of the solar ^{3}He abundance provides an upper limit on the protosolar ^{2}H abundance, which, in turn, provides information on nucleosynthesis in the big bang and on whether the universe is open or closed (Gott et al. 1974).

^{3}He has been observed in the solar wind where the ^{3}He/^{4}He ratio is of the order of a few times 10^{-4} (Geiss and Reeves 1972). Hall (1975) determined spectroscopically a ^{3}He/^{4}He ratio of $(4 \pm 2)\times10^{-4}$ in a solar prominence. There is, however, no direct observation of ^{3}He in the photosphere. The solar gamma-ray observations can set limits on the photospheric ^{3}He abundance. This can be done in two ways. First, for a ^{3}He/H ratio much larger than 5×10^{-5}, the 2.22 MeV line fluence would be much lower relative to the 4 to 7 MeV fluence than observed. Second, the ^{3}He/H ratio must have an upper bound at a value not much higher than 5×10^{-5} because otherwise the delay between neutron production and 2.223 MeV photon release would be shorter than observed. There are as yet no firm values on the upper limits on the ^{3}He/H ratio from the SMM data, but a safe preliminary limit would be $^3\text{He/H} < 2\times10^{-4}$.

In addition to setting an absolute upper bound on the photospheric ^{3}He/H ratio, the gamma-ray data also limit any possible variability of this ratio in time and with position on the solar surface. From the small variability of $\phi(4\text{-}7)/\phi(2.22)$ from flare to flare (Table 2), it follows that ^{3}He/H should be

constant to better than a factor of 2.

As discussed in the Introduction, very high $^3He/^4He$ ratio have been observed in solar energetic particles (see Ramaty et al. 1980 for a review of these observations). It is now believed that these enhancements are not of nuclear origin, but result from selective heating and acceleration (Fisk 1978). Finite $^2H/^1H$ ratios in energetic solar particles averaged over several solar flares have been presented (Anglin, Dietrich and Simpson 1973b, Hurford, Stone and Vogt 1975). But the very large uncertainties in these measurements and the possibility of instrumental contamination preclude a definite conclusion regarding the positive detection of secondary nuclear products in energetic solar particles. It appears, nonetheless, that the bulk of the nuclear reactions are produced by the flare accelerated particles that remain trapped at the Sun. The particles that escape from the Sun and are observed in the interplanetary medium are devoid of any measurable amount of nuclear spallation products.

D. Beaming of the Energetic Particles

As we have seen in Section II D, gamma-ray line observations can give unique information on the beaming of the energetic particles. Shifts in the energies of narrow lines are indicative of such beaming (Ramaty and Crannell 1976), but these effects are probably difficult to measure with low resolution spectrometers. Another effect of beaming is the narrowing of the broad lines. These lines, produced by energetic heavy nuclei, are Doppler broadened by both the velocity spread and the angular distribution of the particles. In the case of a beam, however, the latter effect is greatly reduced and hence broad lines (Figure 9) can mimic narrow lines. For the same reason, the ^7Be and ^7Li lines shown in Figure 13 are much narrower if produced by α-particles

in a beam than by such particles with an isotropic distribution.

The energies of these lines would then provide direct information on the angle between the beam and the direction of observation. A flare model in which the gamma-ray lines would be produced by a beam of energetic particles is that of Colgate (1978). Future gamma-ray line observations and more refined analysis of the SMM data should produce much new information on energetic particles beams in solar flares and hence on the flare model.

IV. SUMMARY

Gamma-ray lines are the most direct probe of nuclear processes in the solar atmosphere. The line observations from a number of flares, made with spectrometers on OSO-7, HEAO-1, HEAO-3 and SMM, are consistent with reactions produced by flare accelerated particles of energies greater than several MeV/nucleon. These reactions involve the production of neutrons, β^+ emitters, π mesons and excited nuclear levels, all of which lead to observable gamma-ray line emission.

The solar gamma-ray line observations can give information on the timing of the nucleonic component in flares, through measurements of the light curves of prompt lines, on the energy spectrum, number and energy content of these particles, through line ratios and line fluences, on the site of the nuclear reactions, through selective attenuation of lines from limb flares and the spectrum and time dependence of e^+-e^- annihilation radiation, on the geometry of particle beams, through line shapes and Doppler shifts, on the photospheric ^3He abundance, through the time dependence and fluence of the 2.223 MeV line, and on chemical compositions of both the ambient medium and the energetic particles, through gamma-ray line ratios.

At the time of this writing (early 1982), only limited portions of the

SMM gamma-ray data are available for analysis and hence only few hard conclusions can be drawn from them (see also Chupp 1982).

The acceleration of protons and nuclei to energies above an MeV, in at least some flares, takes place in a time interval less than a few seconds. This sets important constraints on flare acceleration mechanisms which have not yet been fully explored. For at least some flares, previous ideas on two phases of acceleration, which involve long delays (>1 minute) between the acceleration of MeV nuclei and X-ray producing electrons, are not valid. But there is evidence that the > 10 MeV protons are accelerated later than the < 100 keV electrons.

The 2.223 MeV line is strongly attenuated in limb flares. This provides direct observational confirmation for neutron capture in the photosphere. Further confirmation of this process comes from the precise measurement of the energy of this line (with the high resolution Ge detector on HEAO-3) and from the observed delay between the 2.223 MeV flux and the flux of prompt nuclear radiation. The 2.223 MeV line observations also indicate that the photospheric ^{3}He abundance is about 5×10^{-5} relative to ^{1}H by number, and that it does not vary much with position on the Sun.

The gamma-ray line emission is produced in thick-target interactions, i.e. by energetic protons and nuclei which slow down in the solar atmosphere. The absence of nuclear fragments (^{2}H, ^{3}H, Li, Be, B) in the fluxes of the interplanetary particles indicates that thin-target interactions do not produce many gamma rays. This is probably the reason for the lack of correlation between the number of particles responsible for gamma-ray line production and the number observed in the interplanetary medium.

The ratio of the 4 to 7 MeV photons fluence to the fluence in the 2.223 MeV line is a strong function of the energy spectrum of the accelerated

particles. This spectrum, as deduced from the gamma-ray observations, does not vary much from one flare to another, and is, within rather broad error ranges, similar to the particle energy spectra observed in the interplanetray medium. This argues for the same acceleration mechanism for both the gamma-ray producing particles and the interplanetary particles. In this case, the lack of correlation between the absolute numbers of particles in the two populations could be due to the varying escape conditions of energetic particles from solar flares. Multiple acceleration mechanisms, however, cannot be ruled out at the present time.

Much additional information on solar flares and on energetic particle acceleration therein is expected from the detailed analysis of the already available SMM data and from new data anticipated from the SMM spectrometer as well as from other spectrometers that hopefully will be flown during the next solar maximum toward the end of the 1980's. Of particular interest would be the observation of solar gamma-ray lines with high spectral resolution which could provide unique information on such questions as the beaming of the energetic particles, the temperature of the energetic particle interaction site and the compositions of the ambient medium and the energetic particles.

ACKNOWLEDGMENTS

The author wishes to acknowledge the contributions of B. Kozlovsky, R. E. Lingenfelter and J. M. McKinley to both the calculations and interpretations presented in this paper and Drs. E. L. Chupp, D. Forrest, T. Prince and R. McGuire for providing data prior to their publication. Part of the research described in this paper was supported by NASA's Solar Terrestrial Theory Program.

References

Abramovitz, M. and Stegun, I. A.: 1966, Handbook of Mathematical Functions, Washington, D.C.: U. S. Government Printing Office.

Anglin, J. D., Dietrich, W. F., and Simpson, J. A.: 1973a, in R. Ramaty and R. G. Stone (eds.) High energy Phenomena on the Sun, NASA SP-342, Washington, D. C.: Natl. Aeronautics and Space Administration, p. 315.

Anglin, J. D., Dietrich, W. F., and Simpson, J. A. : 1973b, Astrophys. J. Lett. 186, L41.

Bai, T.: 1982, in R. E. Lingenfelter, H. S. Hudson and D. M. Worrall (eds.) Gamma Ray Transients and Related Astrophysics, New York: Amer. Inst. of Phys., 409.

Bai, T. and Ramaty, R.: 1976, Solar Phys. 49, 343.

Bai, T. and Ramaty, R.: 1979, Astrophys. J. 227, 1072.

Barkas, W. H. and Berger, M. J.: 1964, Tables of Energy Losses and Ranges of Heavy Charged Particles, NASA SP-3013, Washington, D. C.: Natl. Aeronautics and Space Administration.

Bussard, R. W., Ramaty, R. and Drachman, R. J.: 1979, Astrophys. J. 228, 928.

Cameron, A. G. W. : 1981 in C. Barnes, D. D. Clayton and D. N. Schramm (eds.) Essays in Nuclear Astrophysics, Cambridge: Cambridge Univ. (in press).

Cheng, C. C.: 1972, Space Sci. Rev. 13, 3.

Chupp, E. L.: 1976, Gamma Ray Astronomy, Dordrecht:Reidel.

Chupp, E. L.: 1982, in R. E. Lingenfelter, H. S. Hudson and D. M. Worrall (eds.) Gamma Ray Transients and Related Astrophysical Phenomena,New York: Amer. Inst. of Physics, p. 363.

Chupp, E. L. and Forrest, D. J.: 1981, Bull. Amer. Astron. Soc., 13, 909.

Chupp, E. L., et al.: 1973, Nature, 241, 333.

Chupp, E. L., Forrest, D. J., and Suri, A. N.: 1975, in S. Kane (ed.) Solar Gamma X and EUV Radiations, IAU Symp. 68, 341.

Colgate, S. A.: 1978, Astrophys. J., 221, 1068.

Colgate, S. A., Audouze, J., and Fowler, W. A.: 1977, Astrophys. J. 213, 849.

Crannell, C. J., Crannell, H. and Ramaty, R.: 1979, Astrophys. J. 229, 762.

Crannell, C. J., Joyce, G., Ramaty, R., and Werntz, C.: 1976, Astrophys. J. 210, 582.

Croom, D. L. and Harris, L. D. J.: 1973, in H. E. Coffey (ed.) World Data Center Rept. UAG-28 Part I, Collected Data Reports on August 1972 Solar-Terrestrial Events, p. 210.

Dietrich, W. F.: 1973, Astrophys. J. 180, 955.

Dolan, J. F. and Fazio, G. G.: 1965, Rev. Geophys. 3, 319.

Evenson, P., Meyer, P., and Yanagita, S.: 1981, Internat. Cosmic Ray Conference Papers, Paris, 3, 32.

Fireman, E. L., DeFelice, J., and D'Amico, J.: 1976, Proc. Lunar Sci. Conf. 7th., p. 525.

Fisk, L. A.: 1978, Astrophys. J. 224, 1048.

Forman, M. A., Ramaty, R. and Zweibel, E. G.: 1982, (this volume).

Forrest, D. J., Chupp, E. L., and Suri, A.N.: 1975, Proc. Intl. Conf. on X-Rays in Space, Univ. of Calgary, Calgary, Alberta, Canada, p. 341.

Freier, P. S. and Webber, W. R.: 1963, J. Geophys. Res., 68, 1605.

Frost, K. J. and Dennis, B. R.: 1971, Astrophys. J. 165, 655.

Garrard, T. L., Stone, E. C. and Vogt, R. E.: 1973, in R. Ramaty and R. G. Stone (eds.), High Energy Phenomena on the Sun, NASA SP-342, Washington, D. C.: Natl Aeronautics and Space Administration, p. 341.

Geiss, J. and Reeves, H.: 1972, Astronomy and Astrophys. 18, 126.

Gott III, J. R., Gunn, J. E., Schramm, D. N. and Tinsley, B. M.: 1976,

Astrophys. J. 194, 543.

Hall, D. N. B.: 1975, Astrophys. J. 197, 509.

Heitler, W.: 1954, The Quantum Theory of Radiation, London: Oxford Univ. Press.

Hoyng, P., Brown, J. C. and Van Beck, H. F.: 1976, Solar Phys. 48, 197.

Hsieh K. C. and Simpson, J. A.: 1970, Astrophys. J. Letters 162, L191.

Hudson, H. S., Bai, T., Gruber, D. E., Matteson, J. L., Nolan, P. L., and Peterson, L. E.: 1980 Astrophys. J. Letters 236, L91.

Hurford, G. F., Stone, E. C., and Vogt, R. E.: 1975, 14th Internat. Cosmic Ray Conference Papers, Munich, 5, p. 1624.

Ibragimov, I. A. and Kocharov, G. E. 1977, Sov. Astron. Letters, 3 (5), 221.

Kanbach, G., Pinkau, K., Reppin, C., Rieger, E., Chupp, E. L., Forrest, D. J., Ryan, J. M., Share, G. H., and Kinzer, R. L. : 1981, 17th Internat. Cosmic Ray Conference Papers, Paris, (in press).

Kanbach, G. Reppin, C., Forrest, D. J., and Chupp, E. L.: 1975, 14th Internat. Cosmic Ray Conference Papers, Munich 5, 1644.

Kerridge, J. F.: 1975, Science, 188, 162.

Kerridge, J. F., Kaplan, I. R., Lingenfelter, R. E., and Boynton, W. V.: 1977, Proc. Lunar Sci. Conf. 8th, p. 3773.

Kiplinger, A. et al.: 1982, Astrophys. J. (to be published).

Kohl, J. W., Bostrom, C. O. and Williams, D. J.: 1973, in H. E. Coffey (ed.) World Data Center Rept. UAG-28 Part II, Collected Data Reports on August 1972 Solar-Terrestrial Events, p. 330.

Kolata, J. J., Auble, R., and Galonsky, A.: 1967, Phys. Rev. 162, 957.

Kozlovsky, B. and Ramaty, R.: 1974, Astrophys. J. Letters, 191, L43.

Kozlovsky, B. and Ramaty, R.: 1977, Astrophys. Lett. 19, 19.

Lin, R. P. and Hudson, H. S.: 1976, Solar Phys. 50, 153.

Lin, R. P. and Ramaty, R.: 1978 in R. Ramaty and T. L. Cline (eds.) Gamma Ray Spectroscopy in Astrophysics, NASA Tech. Memor. 79619, p. 76.

Lingenfelter, R. E., Flamm, E. J., Canfield, E. H., and Kellman, S.: 1965, J. Geophys. Res. 70, 4077 and 4087.

Lingenfelter, R. E. and Ramaty, R.: 1967, in B.S.P. Shen (ed.) High Energy Nuclear Reactions in Astrophysics, New York: Benjamin, p. 99.

McGuire, R. E., Von Rosenvinge, T. T. and McDonald, F. B.: 1977, 15th Internat. Cosmic Ray Conference Papers, Ploudiv, 5, p. 54.

McGuire, R. E., Von Rosenvinge, T. T. and McDonald, F. B.: 1981, 17th Internat. Cosmic Ray Conference Papers, Paris, 3, p. 65.

Northcliffe, L. C. and Schilling, R. F.: 1970, Nuclear Data Tables A7, 233.

Pesses, M. E., Klecker, B., Gloeckler, G., and Hovestadt, D.: 1981, 17th Internat. Cosmic Ray Conference Papers, Paris, 3, 36.

Pierce, T. E. and Blann, M.: 1968, Phys. Rev. 173, 390.

Prince, T., Ling, J. C., Mahoney, W. A., Riegler, G. R., and Jacobson, A. S.: 1980, Paper presented at the Conference on Cosmic Ray Astrophysics and Low Energy Gamma Ray Astronomy, Univ. of Minnesota, September, 1980.

Ramaty, R.: 1979, in J. Arons, C. Max and C. McKee (eds.) Particle Acceleration Mechanisms in Astrophysics, New York: Amer. Inst. of Physics, p. 135.

Ramaty, R., et al.: 1980 in P. A. Sturrock (ed.) Solar Flares, Boulder, Colorado: Colorado Associated Univ. Press, p. 117.

Ramaty, R. and Crannell, C. J.: 1976, Astrophys. J. 203, 766.

Ramaty, R. and Kozlovsky, B.: 1974, Astrophys. J. 193, 729.

Ramaty, R., Kozlovsky, B., and Lingenfelter, R. E.: 1975, Space Sci. Rev. 18, 341.

Ramaty, R., Kozlovsky, B., and Suri, A. N.: 1977, Astrophys. J. 214, 617.

Ramaty, R. and Lingenfelter, R. E.: 1973 in R. Ramaty and R. G. Stone (eds.) High Energy Phenomena on the Sun, NASA SP-342 Washington, D. C.: Natl. Aeronautics and Space Administration, p. 301.

Ramaty, R., Lingenfelter, R. E., and Kozlovsky, B.: 1982, in R. E. Lingenfelter, H. S. Hudson and D. M. Worrall (eds.) Gamma-Ray Transients and Related Astrophysical Phenomena, New York: Amer. Inst. of Physics, p. 135.

Reppin, C., Chupp, E. L., Forrest, D. J., and Suri, A. N.: 1973, 13th International Cosmic Ray Conference Papers, Denver, Colorado, p. 1577.

Rothwell, P. L.: 1976, J. Geophys. Res. 81, 709.

Schaeffer, O. A. and Zahringer, J.: 1962, Phys. Rev. Letters 8, 389.

Share, G. H.: 1980, Bull. Amer. Astr. Soc., 12, 891.

Suri, A. N., Chupp, E. L., Forrest, D. J., and Reppin, C.: 1975, Solar Phys. 43, 414.

Taylor, H. W., Neff, N. and King: 1967, Phys. Letters 24B, 659.

Van Beek, H. F., Hoyng, P., and Stevens, G. A.: 1973, in H. E. Coffey (ed.) World Data Center Rept. UAG-28 part II, Collected Data Reports on August 1972 Solar-Terrestrial Events, p. 319.

Van Hollebeke, M. A. I., MaSung, L. S., and McDonald, F. B.: 1975, Solar Phys. 41, 189.

Von Rosenvinge, T. T., Ramaty, R., and Reames, D. V.: 1981, 17th Internat. Cosmic Ray Conference Papers, Paris, 3, p. 28.

Wagoner, R. V.: 1973, Astrophys. J. 179, 343.

Wang, H. T.: 1975, 2.2 MeV and 0.51 MeV Gamma-Ray Line Emissions from Solar Flares, Ph. D. Thesis, Univ. of Maryland.

Wang, H. T. and Ramaty, R.: 1974, Solar Phys. 36, 129.

Wang, H. T. and Ramaty, R.: 1975, Astrophys. J. 202, 532.

Webber, W. R., Roelof, E. C., McDonald, F. B., Teegarden, B. J. and Trainor, J.: 1975, Astrophys. J. 199, 482.

Willet, J. B., Ling, J. C., Mahoney, W. A., Riegler, G. R., and Jacobson, A. S.: 1982, in R. E. Lingenfelter, H. S. Hudson and D. M. Worrall (eds.) Gamma Ray Transients and Related Astrophysics, New York: Amer. Inst. of Phys., 401.

TABLE 1

Elemental and Isotopic Abundances

Isotope	Ambient Particles	Energetic Particles
^{1}H	1.	1.
^{4}He	0.07	0.15
^{12}C	4.15×10^{-4}	1.07×10^{-3}
^{13}C	4.64×10^{-6}	1.28×10^{-5}
^{14}N	9.0×10^{-5}	2.14×10^{-4}
^{15}N	3.46×10^{-7}	8.57×10^{-7}
^{16}O	6.92×10^{-4}	2.14×10^{-3}
^{18}O	1.38×10^{-6}	4.28×10^{-6}
^{20}Ne	9.0×10^{-5}	2.14×10^{-4}
^{22}Ne	1.0×10^{-5}	2.57×10^{-5}
^{23}Na	2.28×10^{-6}	4.28×10^{-5}
^{24}Mg	3.11×10^{-5}	6.42×10^{-4}
^{25}Mg	4.01×10^{-6}	8.14×10^{-5}
^{26}Mg	4.43×10^{-6}	8.49×10^{-5}
^{27}Al	3.18×10^{-6}	5.35×10^{-5}
^{28}Si	3.46×10^{-5}	6.42×10^{-4}
^{29}Si	1.80×10^{-6}	3.21×10^{-5}
^{30}Si	1.18×10^{-6}	2.14×10^{-5}
^{32}S	1.80×10^{-5}	1.07×10^{-4}
^{34}S	7.61×10^{-7}	4.71×10^{-6}
^{36}Ar	3.39×10^{-6}	2.14×10^{-5}
^{38}Ar	6.23×10^{-7}	4.28×10^{-6}
^{40}Ca	2.28×10^{-6}	4.28×10^{-5}
^{52}Cr	4.15×10^{-7}	2.14×10^{-5}
^{54}Fe	1.94×10^{-6}	6.85×10^{-5}
^{56}Fe	3.11×10^{-5}	1.07×10^{-3}
^{57}Fe	7.61×10^{-7}	2.57×10^{-5}
^{58}Ni	1.25×10^{-6}	2.14×10^{-5}
^{60}Ni	4.84×10^{-7}	8.57×10^{-6}

Note: Two sets of energetic particle abundances are discussed in the text:
EP1 - Energetic particle abundances given in Column 3.
EP2 - Energetic particles with the same abundances as the ambient medium, Column 2.

TABLE 2

Gamma-Ray Flares

Flare	Fluences, ϕ(photons/cm^2) 2.22 MeV	4-7 MeV	4.44 MeV	6.13 MeV	0.511 MeV	$\frac{\phi(4\text{-}7)}{\phi(2.22)}$	Location
1972, Aug 4	155±12[1]	105±11[2]	17±5[1]	17±5[1]	35±11[1]	0.68±0.09	E08 N14
1972, Aug 7	No data available during time of maximum emission					---	W38 N15
1978, July 11	240±70[3]	171[4]	43±17[3]	---	---	0.71	E43 N18
1979, Nov 9	38±9[5]	50±4[5]	---	---	---	1.32±0.33	E00 S16
1980, June 7	6.6±1[6]	11.5±0.5[6]	---	---	<2	1.74±0.27	W74 N12
1980, June 21	No data available during time of maximum emission*					---	W91 N17
1980, July 1	3.3±0.5[6]	3.1±0.4[6]	---	---	0.9±0.4	0.94±0.19	W37 S12
1980, Nov 6	10.3±1.3[6]	14.8±0.8[6]	---	---	<2	1.44±0.2	E74 S12
1981, Apr 10	13.5±1[6]	18.6±1.6[6]	---	---	<6.6	1.38±0.16	W37 N09
1981, Apr 27	11.7±2[6]	118±2[6]	---	---	---	10.1±1.7	W90 N16

1. Chupp (1975)
2. Ramaty, Kozlovsky and Suri (1977)
3. Hudson et al. (1980)
4. Theoretical
5. T. Prince (private communication 1981)
6. Chupp (1981)

*Delayed 2.22 MeV and 0.511 MeV line, and high-energy neutrons were observed from this flare (Share et al. 1980, Chupp and Forrest 1981).

TABLE 3

Spectral Parameters, Total Energies and Number of Particles of Gamma Ray Flares

Flare	$\bar{f}_n/\bar{f}_n(o)$	$\frac{Q(4-7)}{Q_n}$	αT	W(>1MeV) (erg)	$\bar{N}_p$(>10 Mev)	$N^{obs}_{esc,p}$(>10MeV)
1972 Aug 4	1	0.16	0.019	2.5×10^{30}	1.3×10^{34}	3×10^{35}
1978 July 11	0.9	0.15	0.020	1.8×10^{30}	1.0×10^{34}	---
1979 Nov 9	1	0.30	0.014	9×10^{29}	3.4×10^{33}	---
1980 June 7	0.6	0.24	0.015	2×10^{29}	8.5×10^{32}	10^{31}
1980 July 1	0.95	0.21	0.016	5×10^{28}	2.3×10^{32}	---
1980 Nov 6	0.6	0.20	0.017	2×10^{29}	1.0×10^{33}	---
1981 Apr 10	0.95	0.30	0.014	3.5×10^{29}	1.3×10^{33}	---
1981 Apr 27	~ 0	---	0.019	1.4×10^{30}	7.3×10^{33}	---

TABLE 4

0.511 MeV Line Fluences

Flare	Duration	αT	$Q_+/Q(4-7)$	$\phi(0.51)$(Photons/cm^2) Calculated	Observed
Aug 4, 1972	553 sec	0.019	0.46	48 $\bar{f}_{0.51}$	35±11
June 7, 1980	50 sec	0.015	0.41	4.7 $\bar{f}_{0.51}$	<2
July 1, 1980	60 sec	0.016	0.41	1.3 $\bar{f}_{0.51}$	0.9±0.4
Apr 27, 1981	2000 sec	0.019	0.46	54 $\bar{f}_{0.51}$	<10

Figure Captions

1. Interplanetary protons and α-particles observed on June 7, 1980 (R. McGuire, private communication 1980). The curves are from equation (11) with the same αT for protons and α-particles.
2. Neutron yields in the thin-target and thick-target models calculated with the energetic particle spectra of equation (10) (exponential in rigidity) and equation (11) (Bessel function). The ambient medium and energetic particle compositions are from Table 1. $N_{esc,p}(>E)$ and $N_p(>E)$ are, respectively, the numbers of protons of energies greater than E that escape from the thin-target region or are incident on the thick-target. $n_H T$ is the product of the hydrogen density in the thin-target region and the particle escape time from this region. In the thick-target calculations the particle energy loss rate is given by equation (7) appropriate for for a neutral medium.
3. Partial neutron production rates in the thick-target model for Bessel function energetic particle spectra. The various curves give the neutron production by energetic protons (P), α-particles (α), C, N and O nuclei (CNO) and nuclei from Ne through Fe (Ne-Fe) interacting with the ambient medium. All the other parameters are as in Figure 2.
4. Energy deposition per neutron produced in a thick-target model for Bessel function energetic particle spectra. The various curves give the energy deposited by particles of energies greater than the indicated values. The compositions of the ambient medium and energetic particles are given in Table 1 and the energetic particles are slowing down in a neutral medium.
5. Probabilities for neutron escape, decay, capture on protons and loss on ^3He in the solar atmosphere (solid lines); and photon yields per neutron (dashed lines). The parameter θ is the angle between the Earth-Sun line

and the heliocentric radial direction through the flare. The ratio $^3He/H$ is the photospheric ^3He abundance, and E_n is the energy of the neutrons. The initial neutrons are assumed to be released isotropically above the photosphere (from Wang and Ramaty 1974).

6. The ratio of the positron yield, Q_+, to the neutron yield, Q_n, for Bessel function energetic particle spectra (equation 11). The composition of the ambient medium and energetic particles are given in Table 1 and the energetic particles are slowing down in a neutral medium.

7. The instantaneous fractional positron production rate and the time integrated fractional positron yield in a thin-target model for a burst of β^+ emitter production (δ function) at t = 0. The energetic particles spectrum is given by equation (9) and the compositions are close to those of Table 1. The results of this figure do not depend strongly on the interaction model used.

8. The slowing down time, t_s, plus positronium formation time, t_{pos}, of positrons of initial energies E_+ in an ambient medium of temperature 10^4K, degree of ionization n and density 10^{11} or 10^{13} cm^{-3}. At the linear parts of the curves, $t_s >> t_{pos}$; t_s is essentially independent of temperature and does not depend much on n; t_{pos}, however, depends strongly on these parameters (see Bussard, Ramaty and Drachman 1979 for more details). The calculations of Figure 8 have been carried out by J. M. McKinley (private communication 1981).

9. Prompt nuclear gamma-ray spectrum from the interactions of energetic particles with the solar atmosphere in a thin-target model. The composition of the ambient medium is given in Table 1. The energy spectrum of the energetic particles is given by equation (9) and their composition is the same as that of the ambient medium (EP2). Not shown in this figure

are the delayed lines, at 2.223 MeV from neutron capture and at 0.511 MeV from positron annihilation. In the August 4, 1972 flare, these lines were ~ 10 and 2 times more intense, respectively, than the ^{12}C line at4.44 MeV. (From Ramaty et al. 1980).

10. The ratio of the narrow 4.44 MeV line yield to the neutron yield for energetic particle spectra given by equation (11). The compositions of the ambient medium and energetic particles are given in Table 1.
11. The ratio of the photon yield in the 4 to 7 MeV channel to the neutron yield for energetic particle spectra given by equation (11). The composition of the ambient medium is given in Table 1. The curves EP1 are for energetic particles of composition as given in Table 1 while the curves EP2 are for an energetic particle composition which is the same as that of the ambient medium in Table 1.
12. The ratio of the narrow 4.44 MeV line yield to the 4 to 7 MeV channel yield. The rest of the parameters are the same as in Figure 11.
13. Photon spectrum of the prompt ^{7}Li and ^{7}Be lines for an α-particle beam confined to a cone with half opening angle 5° or 20°, and for an isotopic distribution; θ_0 is the angle between the beam and the direction of observation. (From Kozlovsky and Ramaty 1977).

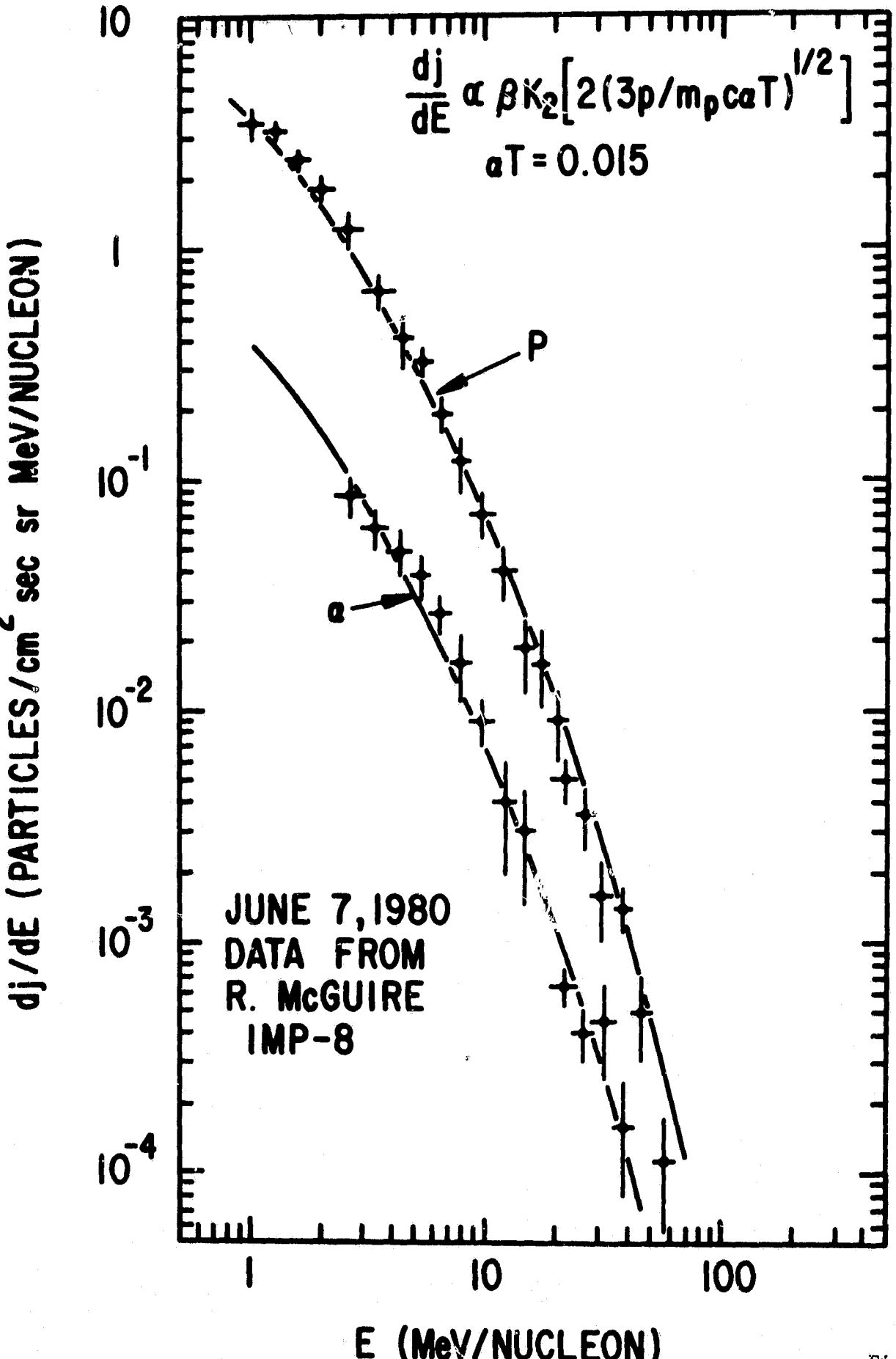
$\frac{dj}{dE} \propto \beta K_2[2(3p/m_p c\alpha T)^{1/2}]$
$\alpha T = 0.015$
P
α
JUNE 7, 1980
DATA FROM
R. McGUIRE
IMP-8
dj/dE (PARTICLES/cm² sec sr MeV/NUCLEON)
E (MeV/NUCLEON)
10
1
10⁻¹
10⁻²
10⁻³
10⁻⁴
1
10
100

Figure 1

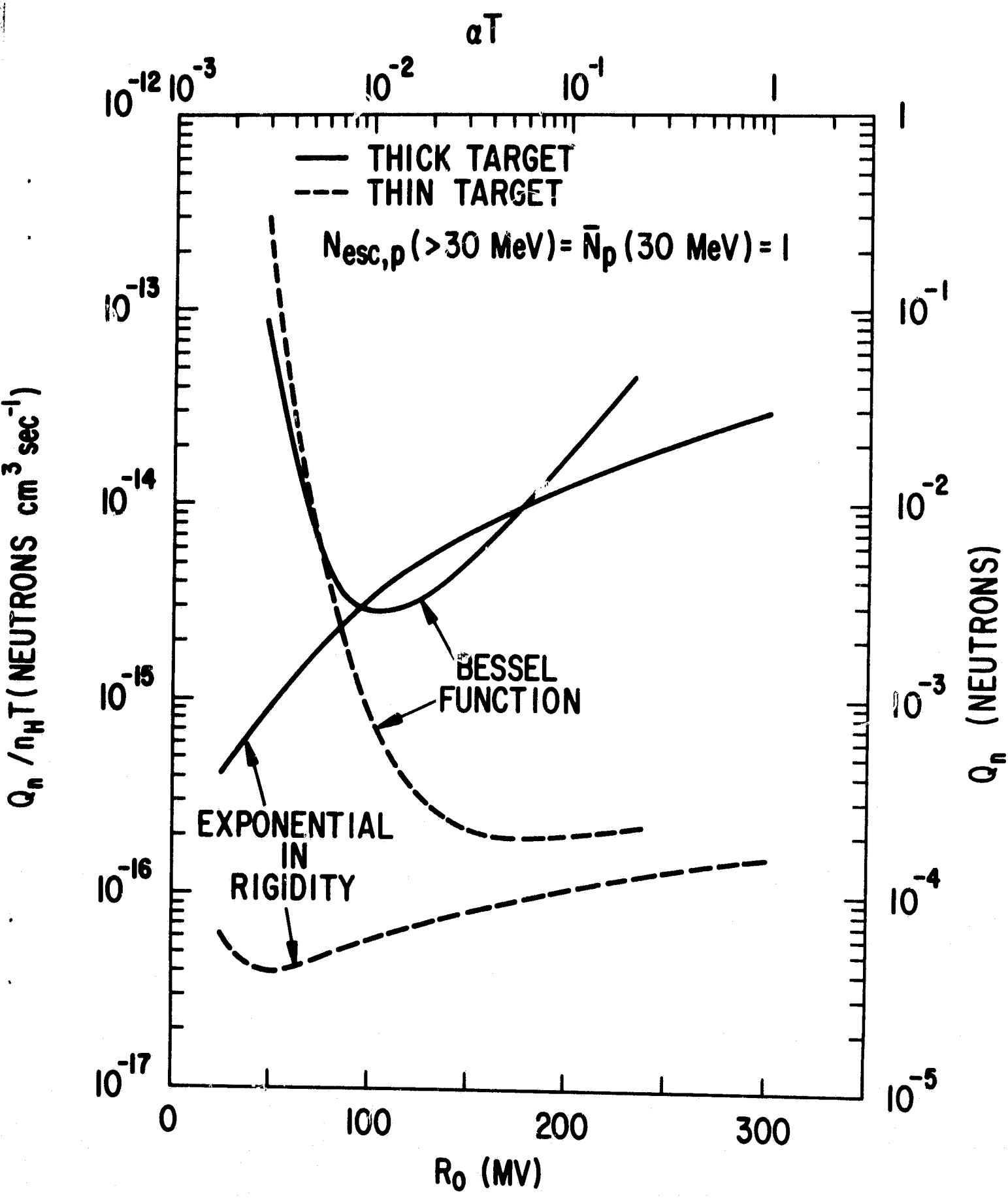
αT
10^-3
10^-2
10^-1
1
10^-12
10^-13
10^-14
10^-15
10^-16
10^-17
THICK TARGET
THIN TARGET
N_esc,p (>30 MeV) = N̄_p (30 MeV) = 1
BESSEL FUNCTION
EXPONENTIAL IN RIGIDITY
Q_n /n_H T (NEUTRONS cm^3 sec^-1)
Q_n (NEUTRONS)
10^-1
10^-2
10^-3
10^-4
10^-5
0
100
200
300
R_0 (MV)

Figure 2

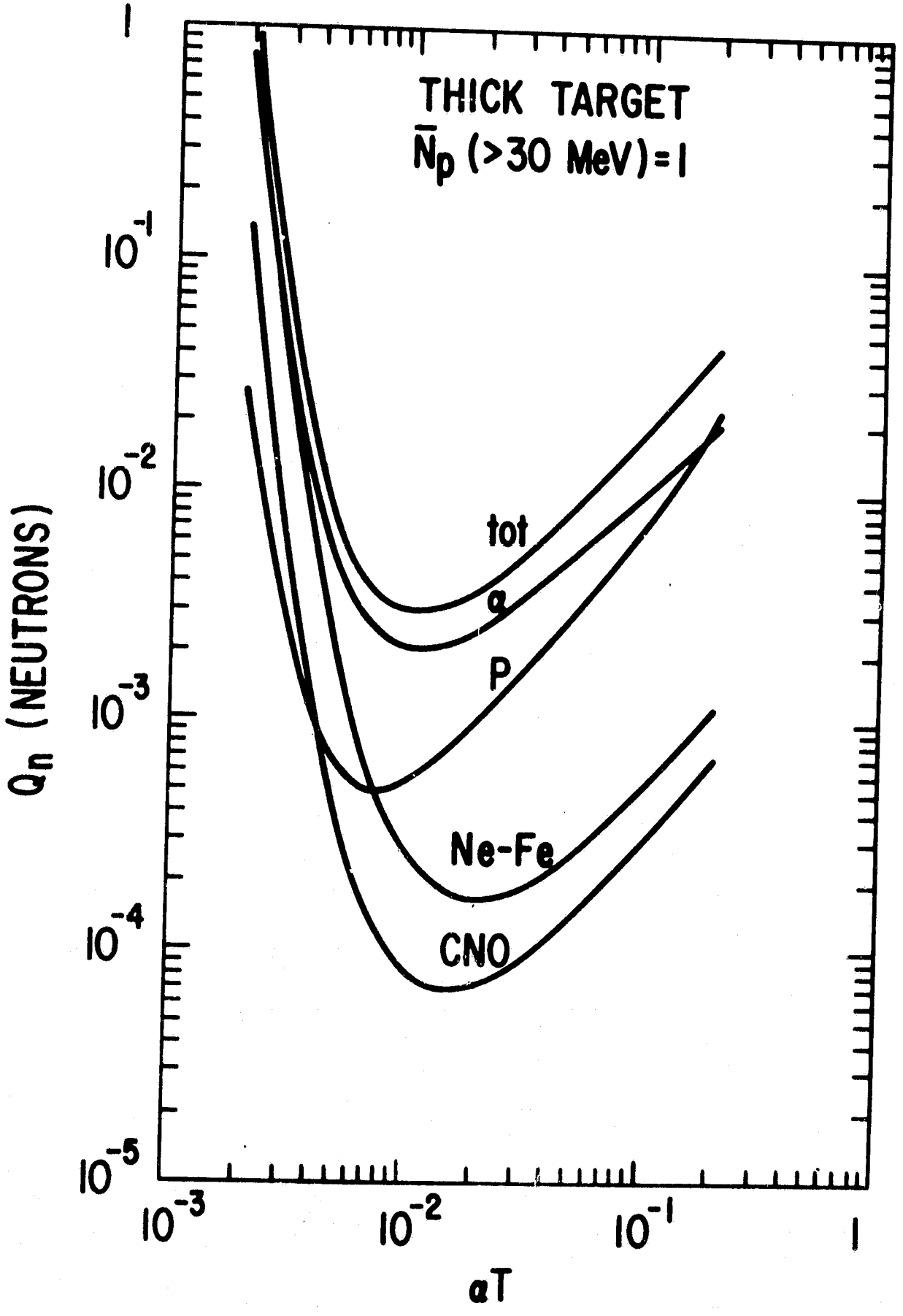
THICK TARGET
$\bar{N}_p$ (>30 MeV)=1
tot
α
P
Ne-Fe
CNO
Q_n (NEUTRONS)
αT
1
10^{-1}
10^{-2}
10^{-3}
10^{-4}
10^{-5}
10^{-3}
10^{-2}
10^{-1}
1

Figure 3

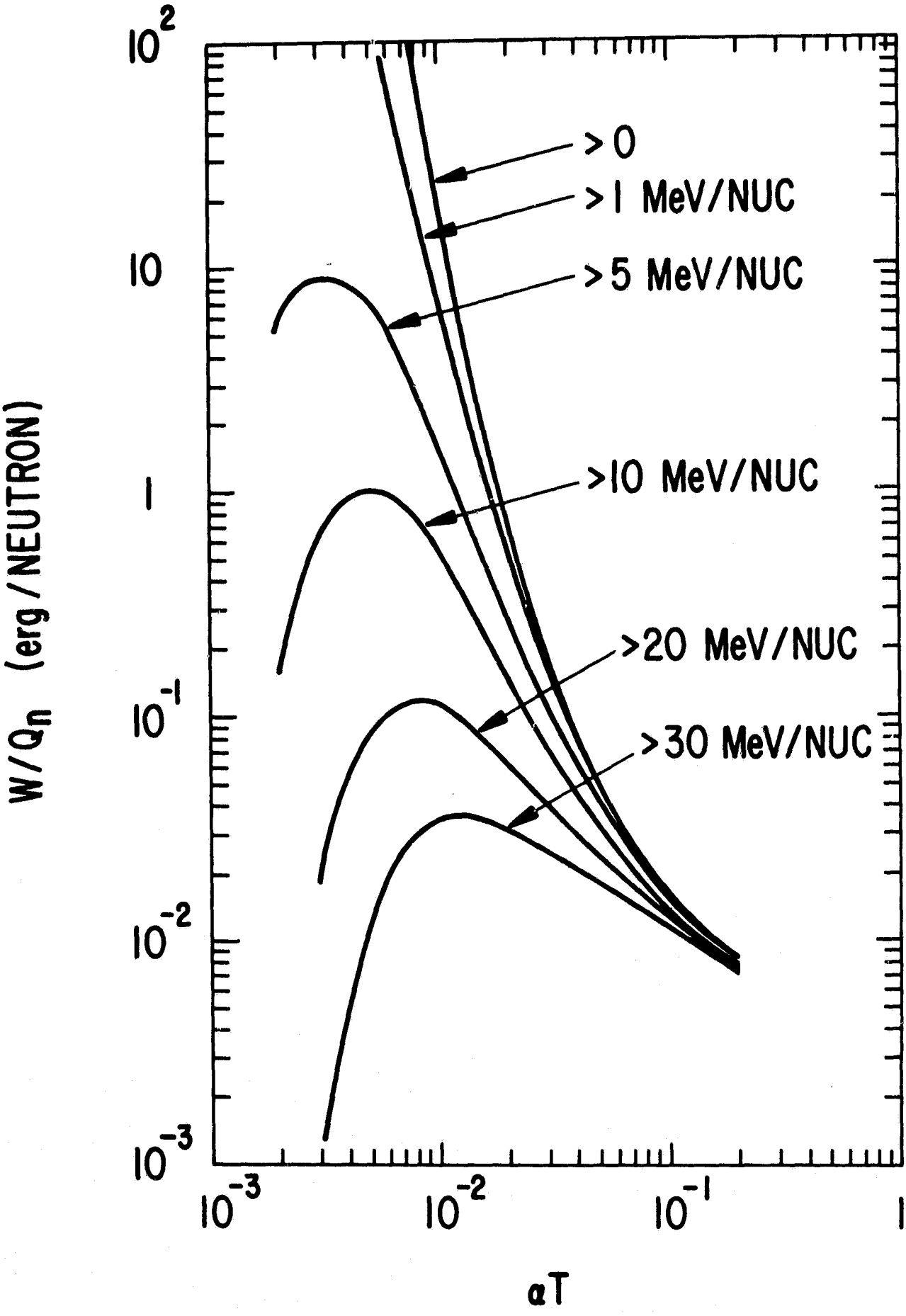
10^2
10
1
10^{-1}
10^{-2}
10^{-3}
W/Q_n (erg/NEUTRON)
>0
>1 MeV/NUC
>5 MeV/NUC
>10 MeV/NUC
>20 MeV/NUC
>30 MeV/NUC
10^{-3}
10^{-2}
10^{-1}
1
αT

Figure 4

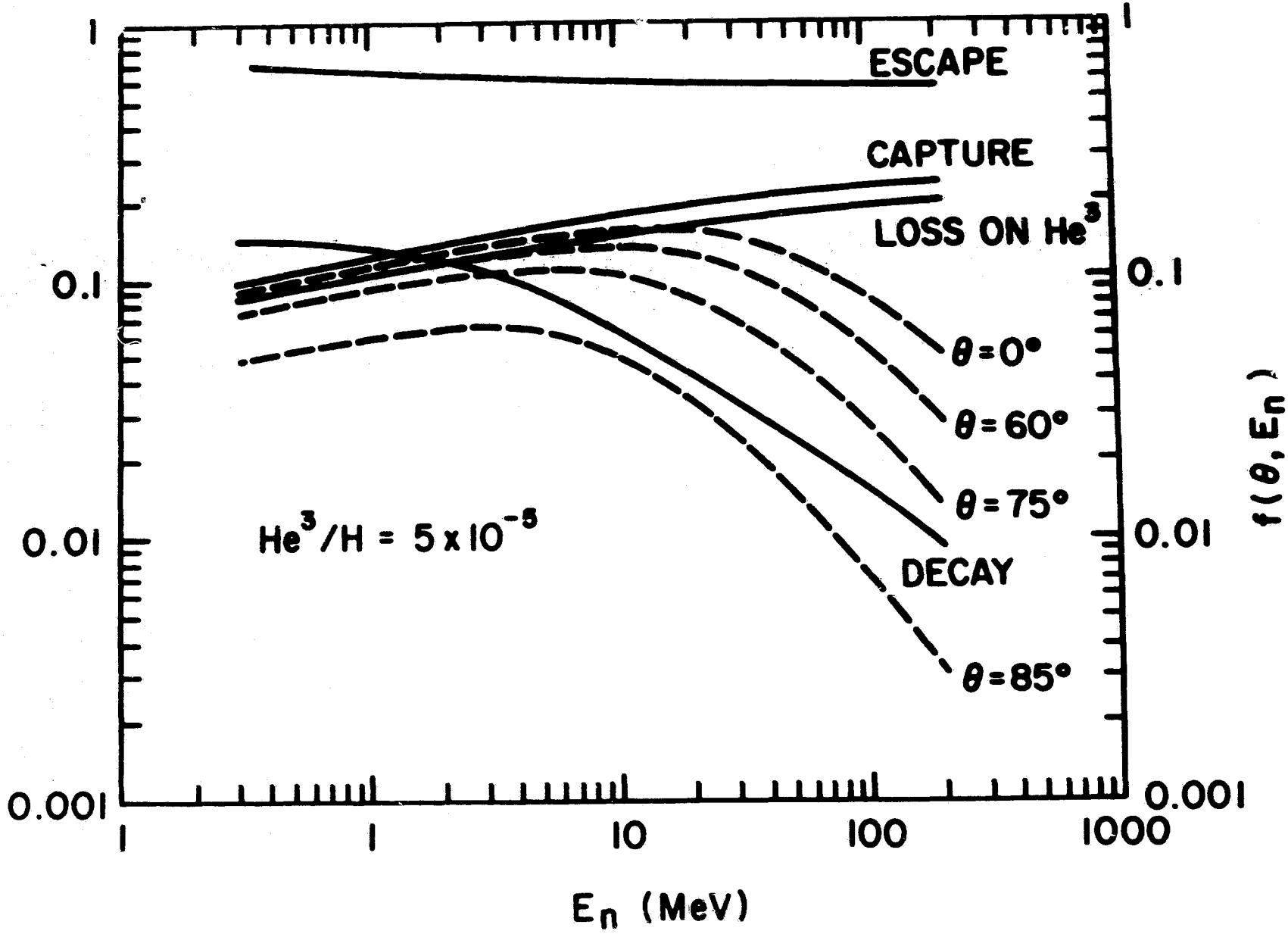
ESCAPE
CAPTURE
LOSS ON He³
θ=0°
θ=60°
θ=75°
θ=85°
DECAY
He³/H = 5 x 10⁻⁵
PROBABILITY
f(θ, En)
En (MeV)
1
0.1
0.01
0.001
1
10
100
1000

Figure 5

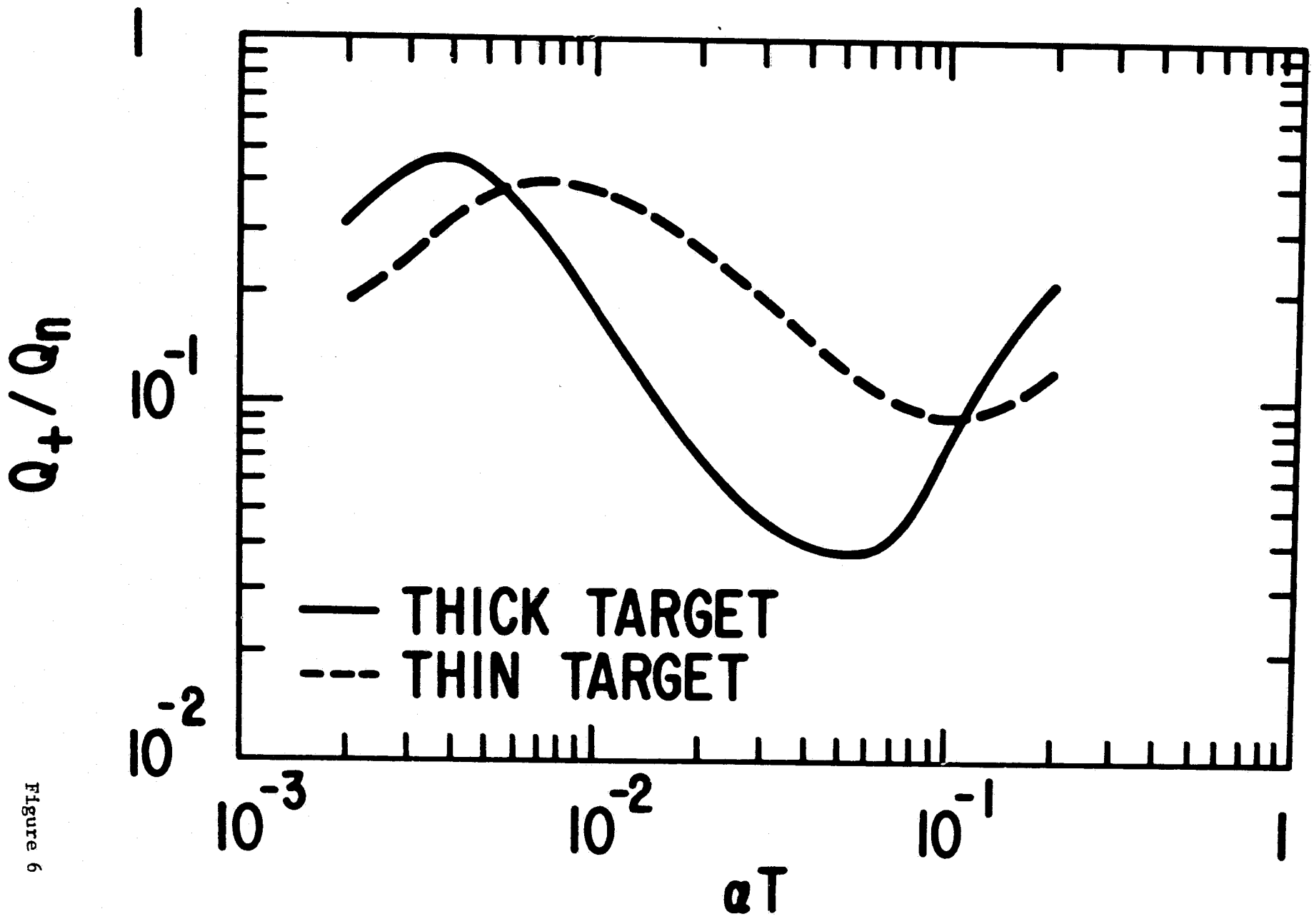

Figure 6

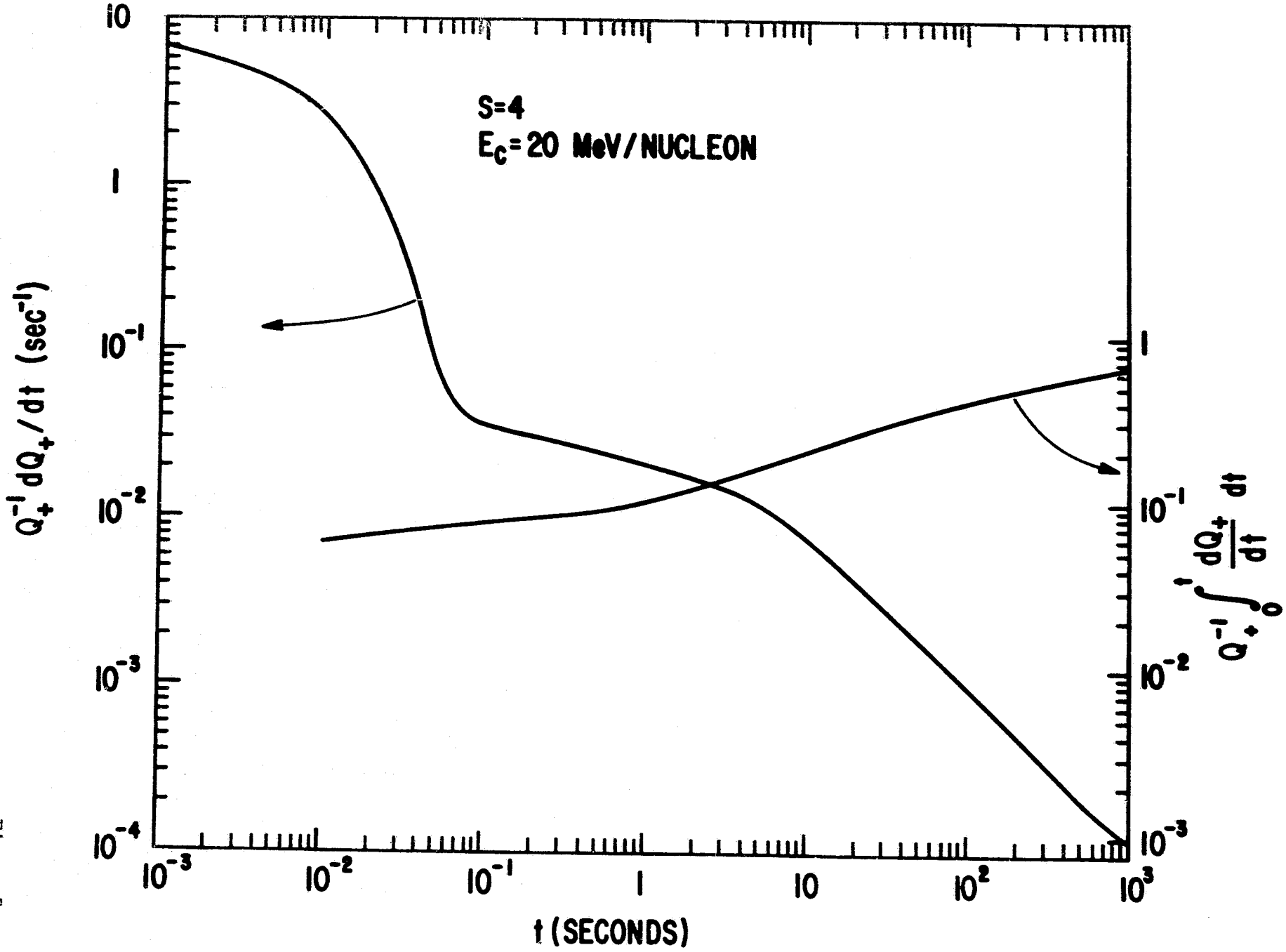
S=4
E_c=20 MeV/NUCLEON
$Q_+^{-1} dQ_+/dt$ (sec^{-1})
$Q_+^{-1} \int_0^t \left|\frac{dQ_+}{dt}\right| dt$
t (SECONDS)
10
1
10^{-1}
10^{-2}
10^{-3}
10^{-4}
10^{-3}
10^{-2}
10^{-1}
1
10
10^2
10^3

Figure 7

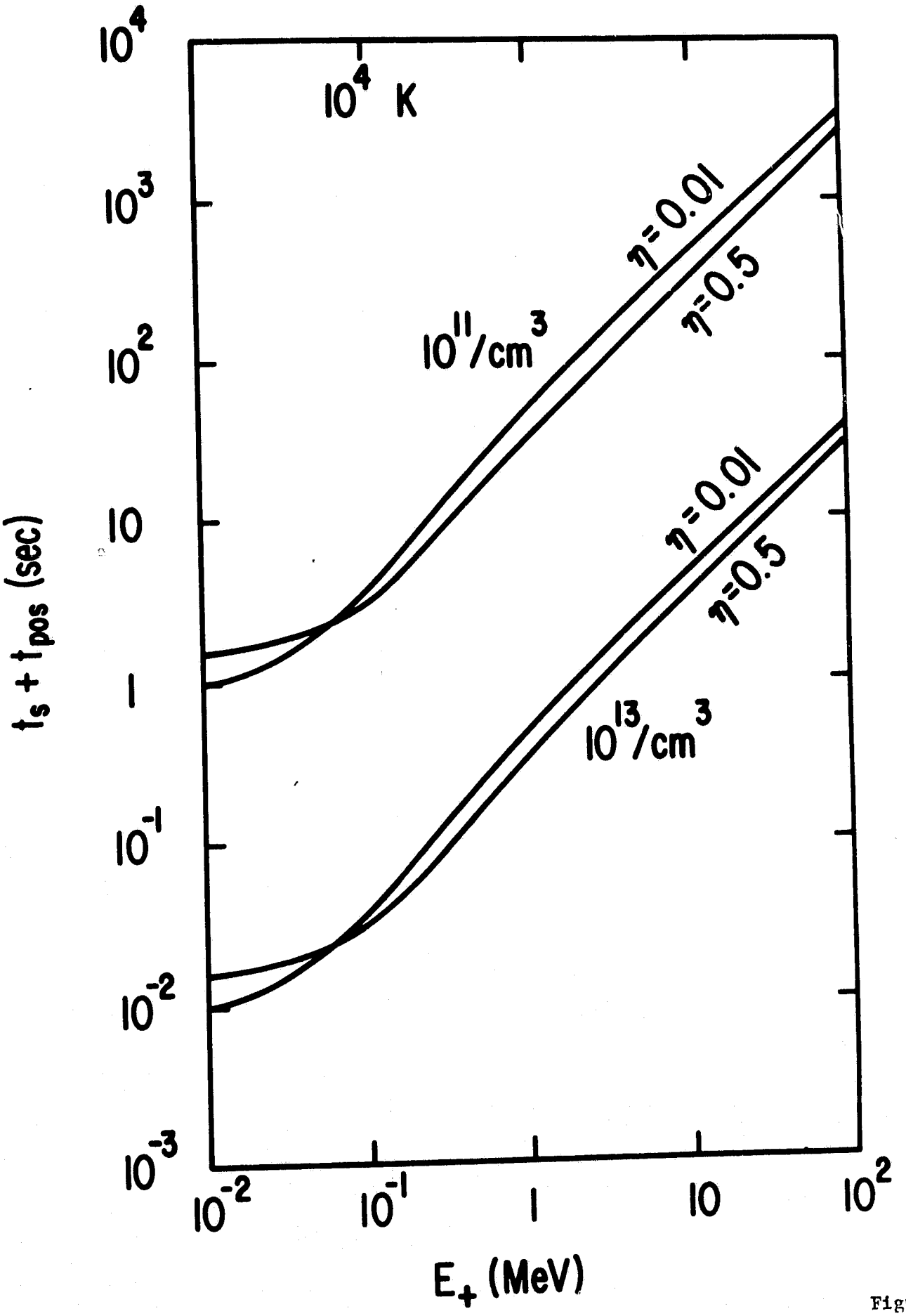
10^4 K
10^{11}/cm^3
10^{13}/cm^3
η=0.01
η=0.5
η=0.01
η=0.5
$t_s + t_{pos}$ (sec)
E_+ (MeV)
10^4
10^3
10^2
10
1
10^{-1}
10^{-2}
10^{-3}
10^{-2}
10^{-1}
1
10
10^2

Figure 8

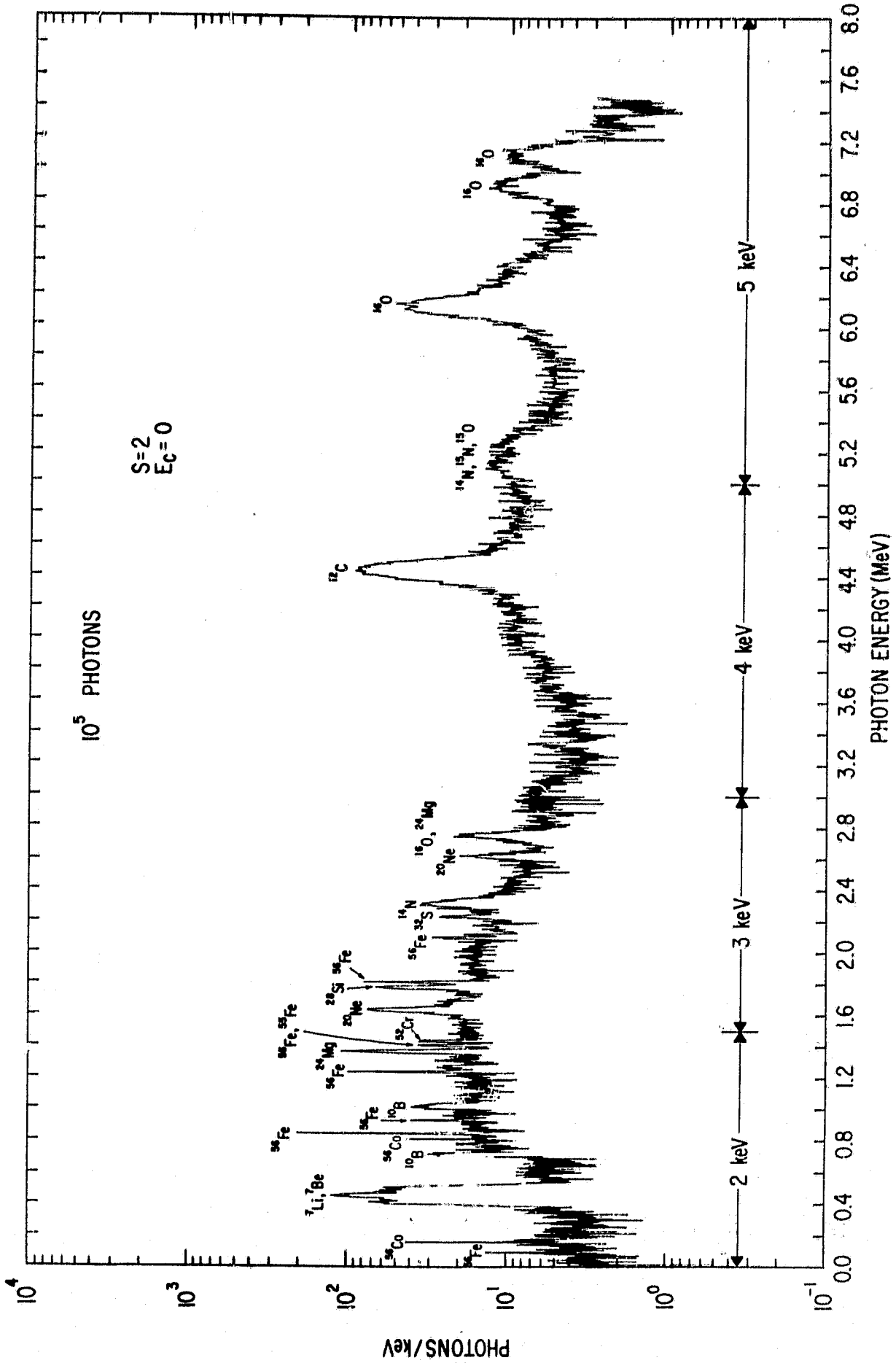
PHOTONS/keV
PHOTON ENERGY (MeV)
10^5 PHOTONS
S=2
E_c=0
2 keV
3 keV
4 keV
5 keV
^{12}C
^{16}O
^{14}N, ^{15}N, ^{15}O
^{16}O, ^{24}Mg
^{20}Ne
^{14}N
^{56}Fe ^{32}S
^{28}Si ^{56}Fe
^{20}Ne
^{52}Cr
^{56}Fe, ^{55}Fe
^{24}Mg
^{56}Fe
^{56}Fe
^{10}B
^{56}Co
^{10}B
^{56}Fe
^{7}Li, ^{7}Be
^{56}Co
^{56}Fe

Figure 9

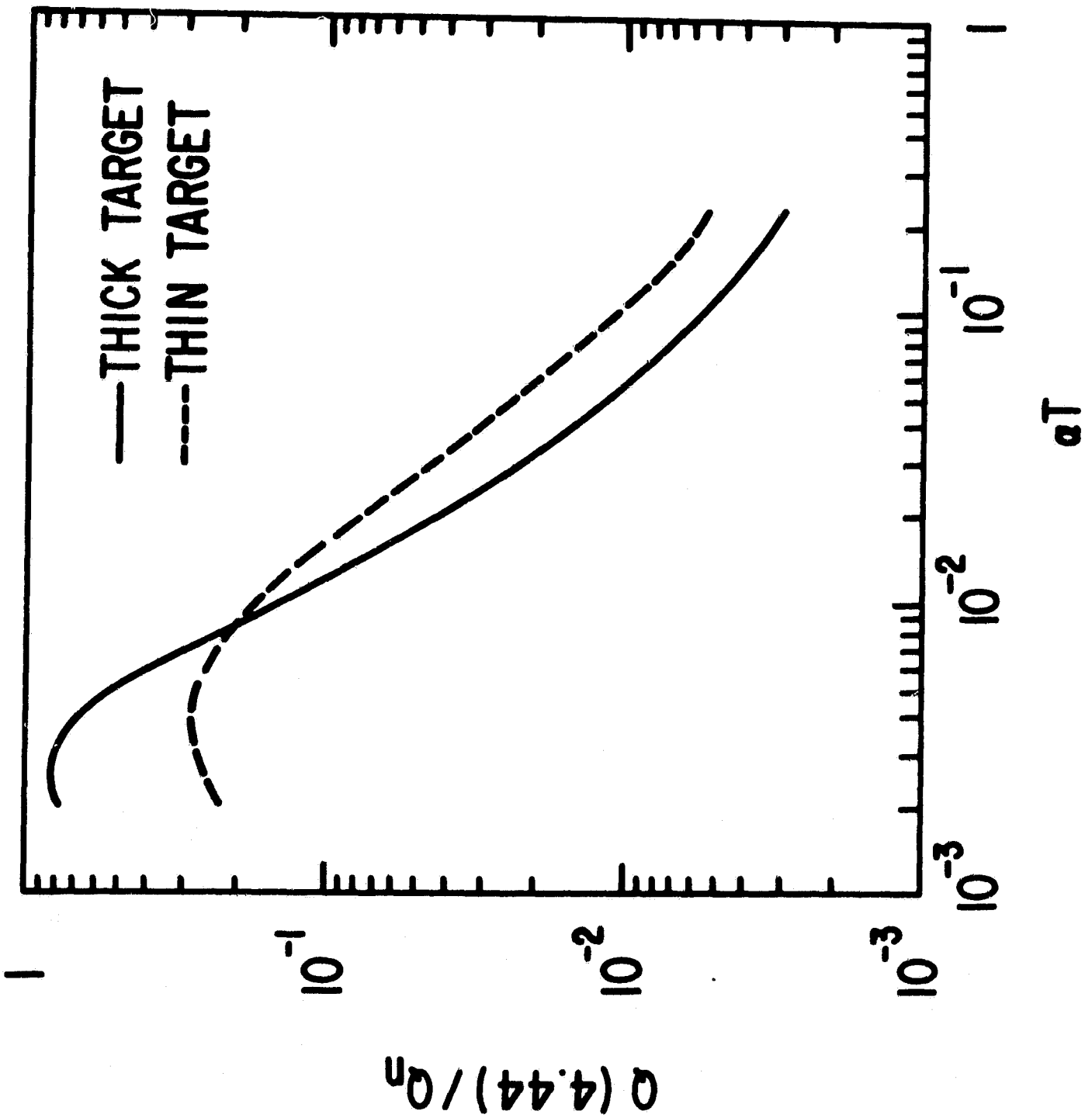

Figure 10

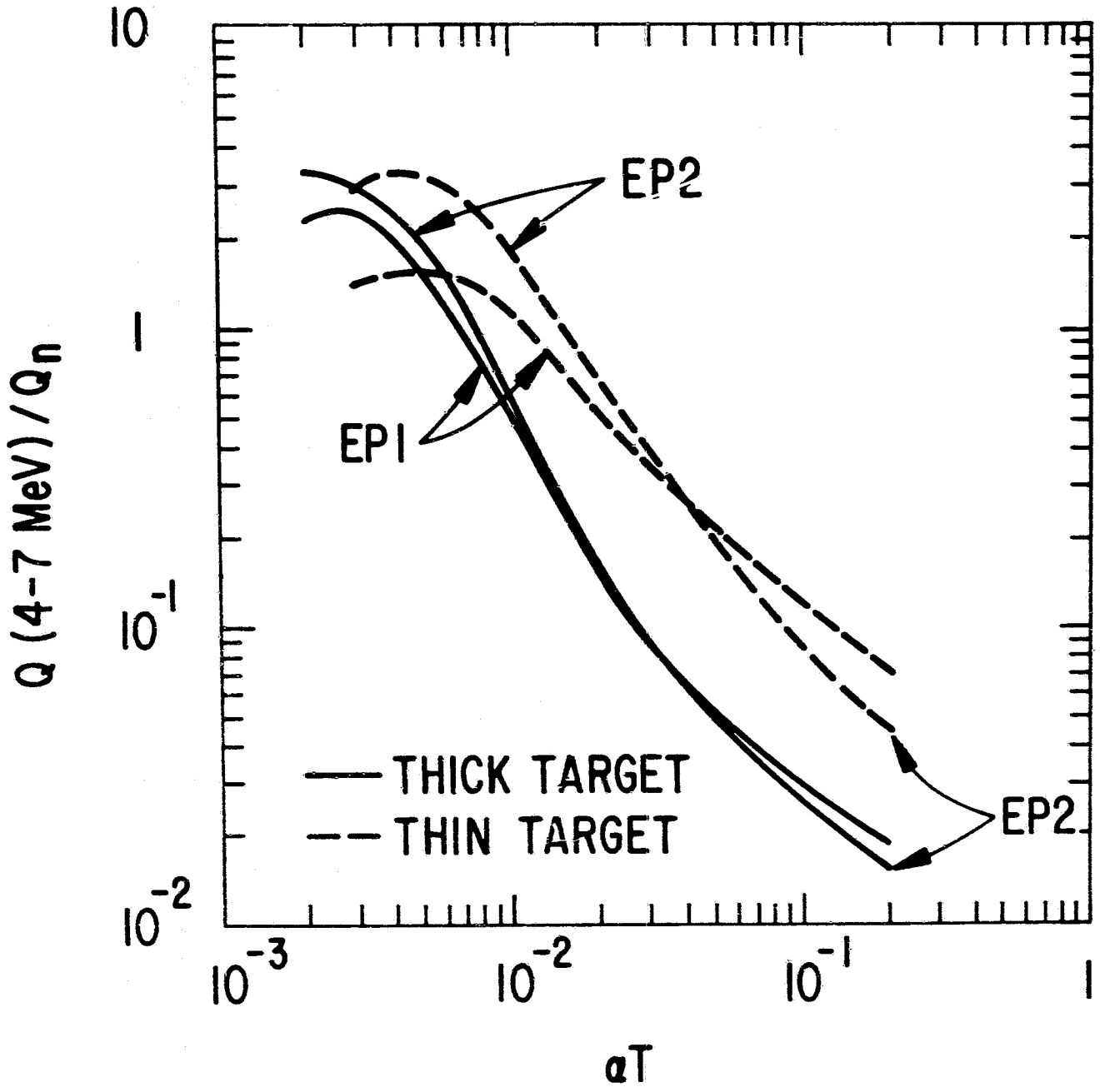
10
1
10^{-1}
10^{-2}
Q (4-7 MeV) / Q_n
EP2
EP1
EP2
THICK TARGET
THIN TARGET
10^{-3}
10^{-2}
10^{-1}
1
αT

Figure 11

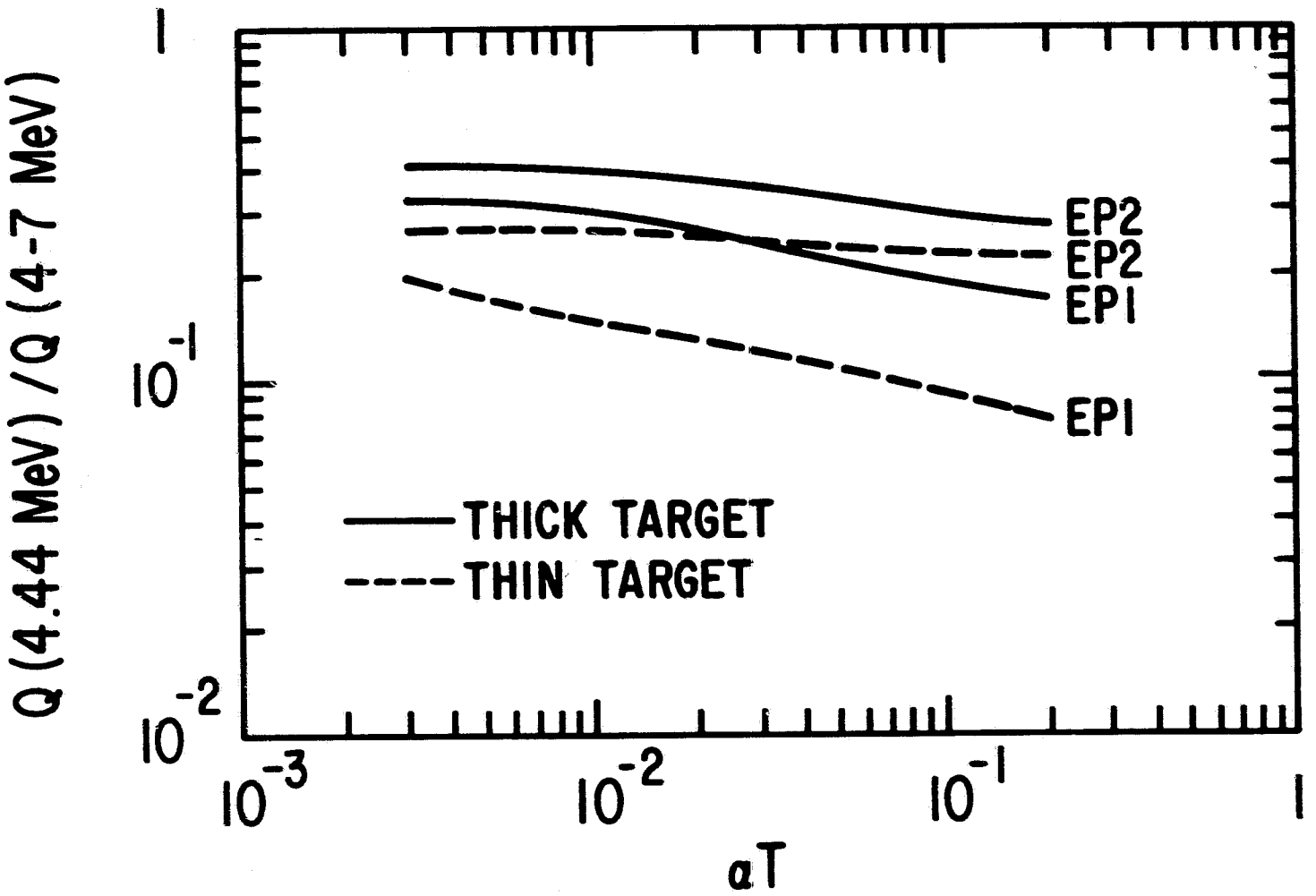
Q (4.44 MeV) /Q (4-7 MeV)
1
10^{-1}
10^{-2}
10^{-3}
10^{-2}
10^{-1}
1
αT
EP2
EP2
EP1
EP1
THICK TARGET
THIN TARGET

Figure 12

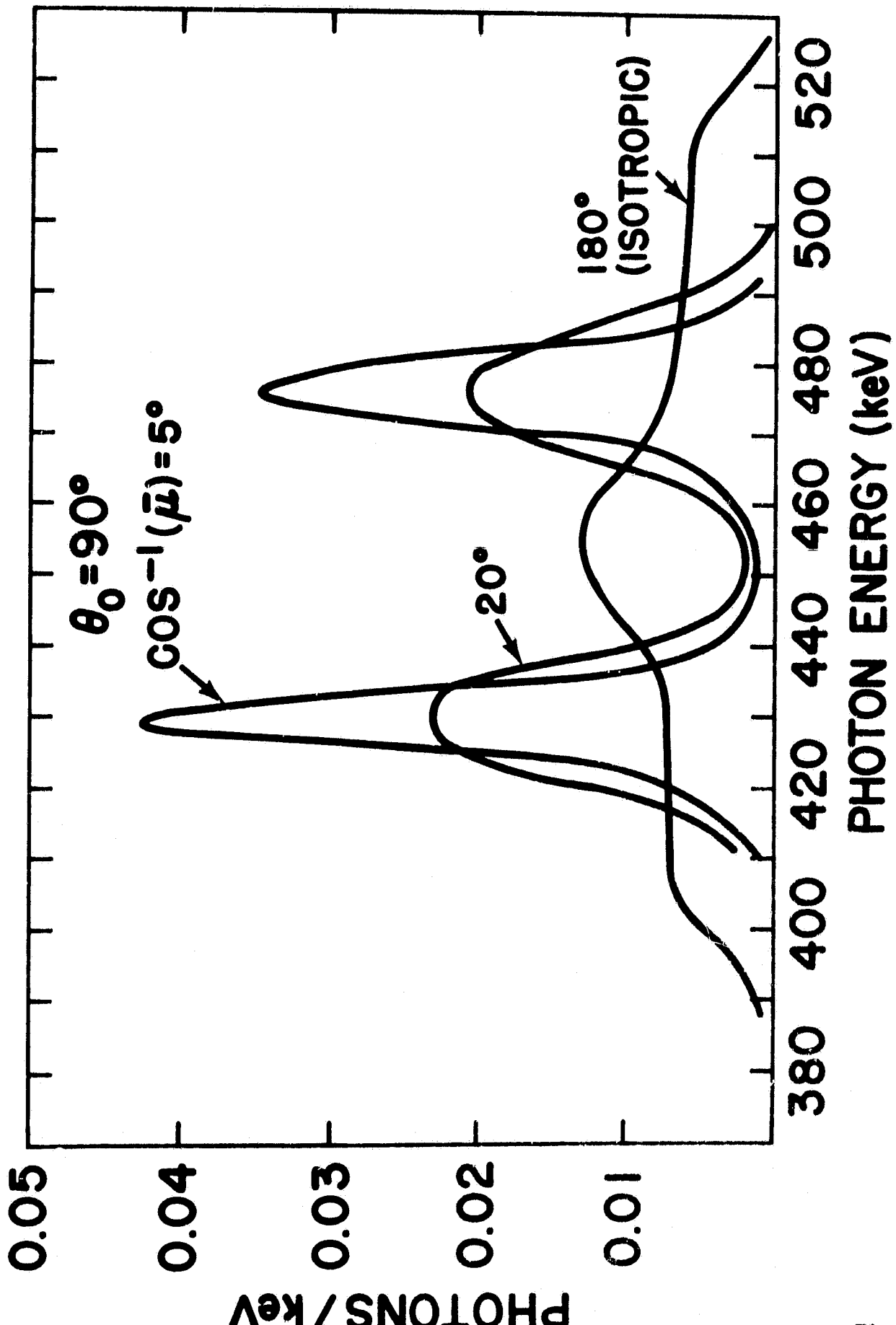
PHOTONS / keV
0.05
0.04
0.03
0.02
0.01
380
400
420
440
460
480
500
520
PHOTON ENERGY (keV)
$\theta_0 = 90°$
$\cos^{-1}(\bar{\mu}) = 5°$
20°
180° (ISOTROPIC)

Figure 13